Addis Ababa University

Addis Ababa Institute of Technology

School of Mechanical and Industrial Engineering

(Mechanical Design Stream)

Analysis of Wear Resistance of Wheel-Rail Contact Surface Materials: In the Case of Addis Ababa Light Rail Transit

A Thesis Submitted to the School of Graduate Studies of Addis Ababa University in Partial Fulfillment of the Requirements for the Degree of Masters of Science in Mechanical Engineering

By

Name: Teshome Meku Godie

Advisor: Dr. Daniel Tilahun

Co-advisor: Mr. Muluken Masresha (PhD Candidate)

January, 2020

Addis Ababa, Ethiopia

Addis Ababa University

Addis Ababa Institute of Technology

School of Mechanical and Industrial Engineering

Analysis of Wear Resistance of Wheel-Rail Contact Surface Materials: In the Case of Addis Ababa Light Rail Transit

(Mechanical Design Stream)

By

Teshome Meku Godie

A Thesis Submitted to the School of Graduate Studies of Addis Ababa University in Partial Fulfillment of the Requirements for the Degree of Masters of Science in Mechanical Engineering

Approved by Board of Examiners:

Dr. Daniel Tilahun Advisor	____________ Signature	____________ Date
Mr. Tolossa Deberie External Examiner	____________ Signature	____________ Date
Dr. Samuel Tesfaye Internal Examiner	____________ Signature	____________ Date
Dr. Yilma Tadesse Chair Person	____________ Signature	____________ Date

Declaration

I hereby declare that the work which is being presented in this thesis entitled **“Analysis of Wear Resistance of Wheel-Rail Contact Surface Materials: In the Case of Addis Ababa Light Rail Transit”** is my original work, has not been presented for a degree of any other university and all the resource materials used for this thesis have been duly acknowledged.

Teshome Meku	______________	____________________
Name	Signature	Date

Acknowledgment

First, I would like to thank God for giving me health with his endless love and support. Next, I would like to express my deepest gratitude to my adviser, Dr. Daniel Tilahun for his interest in this thesis from the very early stage of this thesis work and giving me his helpful comments and suggestions. My special thanks also go to my co-advisor Mr. Muluken Masresha for giving me his helpful comments and suggestions continuously and without his advises, encouragement and patience; this work would not have been possible. The suggestions, tips and advises given by my friend Natnael Tesfamichael were immensely helpful in modeling the railway wheel and rail components. Additionally, I want to express my gratitude to Metals and Engineering Corporation (METEC) and Ethiopian Railway Corporation (ERC) staff members, experts and technicians for their valuable assistance in this thesis work. I would like to express my sincere thanks to all my classmates for their undivided assistance and attitude to strengthen me throughout this work.

Finally, I would like to thank my dear wife Mekdes Demeke for her continuous support and great encouragement.

Abstract

The purpose of this thesis is to study wear resistance of wheel-rail contact materials of Manganese steel and Pearlite steel. The wheel-rail contact is a critical interface in the railway technology and study of failures in most railways may cause due to wear of wheel-rail contact surfaces. Application of this thesis is on railway technology in the specific area of Addis Ababa Light Rail Transit. It is a new railway technology in Ethiopia. So researches on this area are needed to identify the existing problems and to avoid such problems from the start.

The method of this thesis is numerical and analytical analysis of wear resistance of Manganese and Pearlite steels. Based on this method wear and wear resistance of wheel-rail contact materials are evaluated.

Using the results of wear and wear resistance of Manganese Steel (current material of Addis Ababa Light Rail Transit) is compared with Pearlite Steel (new material). Since, wear volume of Manganese steel and Pearlite is 0.00169 m^3 and 0.00141m^3 respectively at maximum load and maximum distance traveled and wear rate value of Manganese steel is 0.00000335 m^3/m and Pearlite steel is 0.00000205m^3/m. On the other hand wear resistance value of Manganese steel and Pearlite steel is 3.98e^5 and 4.88e^5 m/m^3 respectively. And also wear index value of Manganese steel is 1846.43 and 1599.97 for Pearlite steel. Results of this wear analysis shows that there is less amount of wear volume, wear rate and wear index in Pearlite steel than Manganese steel. On the other hand wear resistance of Pearlite steel has higher than Manganese steel. Finally, this thesis verified that Pearlite steel is better in hardness than Manganese steel.

Key words: wheel-rail contact; wear; wear resistance; hardness.

Table of Contents

List of Acronyms

AALRT: Addis Ababa Light Rail Transit

AAR: Association of American Railroad

ABMI: Akaki Basic Metals Industry

AISI: American Iron and Steel Industry

ASTM: American society for Testing and Materials

BHN: Brinell hardness number

BS: British Standard

COF: Coefficient of friction

EN: European standard

ERC: Ethiopian Railway Corporation

E_w and E_r: Young's Modulus of the railway Wheel and Rail Material

FEM: Finite Element Method

F_N: Normal Load at the Wheel/rail Contact

GUI: Graphical User Interface

HMMBI: Hibret Manufacturing and Machine Building Industry

H_r: Hardness of rail

H_w: Hardness of wheel

JIS: Japanese Industrial Standard

K: wear coefficient

K_w: Constants that depend on the material properties of wheel.

K_r: Constants that depend on the material properties of rail.

K_3: Geometrical Properties of both Wheel and Rail.

a: Major Semi-axis

b: Minor Semi-axis

METEC: Metals and Engineering Corporation

m and n: Hertz coefficients

P: Contact Pressure

Po: Maximum Contact Pressure

R_{1w}: The Principal Rolling Radii of the Wheel

R_{2w}: The principal transverse radii of the wheel

R_{1r}: The principal rolling radii of the rail

R_{2r}: The principal transverse radii of the rail

RCF: Rolling contact fatigue

S: sliding distance

S_d: Flange Thickness

SN: Stress against the number of cycles to failure

T_d: Thread Diameter

UIC: International Union of Railways

v_w and v_r: Poisson's ratio of Wheel and rail Material

W_v: Wear Volume

WB: Workbench

List of Tables

List of Figures

CHAPTER ONE: INTRODUCTION

1.1. Background

The wear at the wheel-rail interface is a critical problem in railway field. Railway transportation is a very important transportation system in worldwide transport and has several advantages on motorway transportation from the view point of environmental impact [1]. Wear can be defined as the surface damage or the removal of material from solid surfaces by mechanical action and it is a natural phenomenon that exists when two bodies are in contact. Wear can appear in many ways, depending on the material of the interacting contact surfaces, the operating environment and the running conditions [2]. On the other hand, wear occurs in many ways. Such as due to rolling/sliding contact, contact of a particle with solid materials and repeated (cyclic) contacts of materials and this is true for the wheel and rail of a railway vehicle. This type of wear is mainly dependent on the type of materials used in the wheel-rail surface [3]. Therefore, to know these losses of materials, wear resistant of material properties are analyzed. These analyses also helps to get better understanding of materials that have the resisting capacity of loads and stresses at different points of wheel-rail contact surface.

A large body of empirical data has been collected and some phenomenological models have been developed on wear of materials. The first experimental investigations of wear have been carried out by Hatchett (1803) and Rennie (1829). In our days, experimental tests of wear intensities of materials belong to standard measurements of mechanical properties of solids. Contacting elements of structures are very common in technology. Many mechanical devices and mechanisms are constructed with the aid of component parts contacting one with another. Loads, motions and heat are transmitted through the contacts of structures. Friction and wear accompany any sliding contact. Nevertheless, it is difficult to predict and to control wear of rubbing elements i.e. wear cannot be totally prevented [4]. It has been widely acknowledged that railway wheels and rails suffer surface damages such as wear and rolling contact in service process of wheel/rail interaction. Although rail/wheel lubrication and material improvement have considerably decreased the wear rate of both elements, wear may be still a comparatively great problem [5]. The life of railway wheels is usually limited by wear. The wheel surface is subjected to high normal and tangential contact stresses. Contact forces change magnitude and orientation as the wheel travels over the rail curves, crossings and local surface perturbations. This constantly changing contact patch moves over the wheel tread and to a certain extent of the flange. The contact between wheel and rail is nominally rolling but a small amount of local sliding takes place at the interface. The amount of sliding depends on the contact patch geometry, normal force, lateral force and friction coefficient [6].

In many well lubricated contacts adhesion between the two surfaces is negligible, yet there is still a significant rate of wear. This wear is caused by deformations sustained by the asperities and surface layers when the asperities of opposing surfaces make contact. Contacts between asperities accompanied by very high local stresses are repeated a large number of times in the course of sliding or rolling and wear particles are generated by fatigue wear. When an elastic body, such as a wheel, is pressed against another elastic body, such as a rail, so that a normal load is transmitted, a contact area is formed. The wheel and rail contact interaction are mainly affected by geometry of the bodies, inputs of material parameters and applied loads [7-9].

There are different lists of materials for the rail and wheel of a train, which have been discovered by different researchers. All these materials are steel based but with different hardness, grain structure and other mechanical properties. We can select high wear resistance materials like pearlite steels or by taking material combination of wheel & rail; ER7 for the wheel and 60E1 for the rail. These materials are recently used in Europe [10]. The main idea of this study is to know the cause of wear in the wheel-rail contact and evaluate the wear resistance.

Stress in wheel-rail contact is the key to understand and predict the damage mechanisms of wheel and rail. According to Journal of Ekberg(2014) "The contact between wheel and rail generates stresses which leads to wear of materials". Therefore, it is necessary to investigate stresses in wheel and rail contact. The contact section between the rail and rail road wheel are extremely stressed due to load of vehicles and passengers [11].

1.2. Statement of the Problem

Wheel and rail are always in contact which leads to wear of materials. Wear has a significant effect on wheel and rail components in the case of AALRT. The wheels are promised to serve more than 5 years depending on the track design and operational conditions. Therefore, better wear resistant materials of wheel-rail contact surfaces are needed to achieve this wheel service. So, in this study wheel-rail contact materials of AALRT are used to make wear analyses. This thesis focuses on analysis of wear resistance of wheel-rail contact materials. Wear analysis of wheel and rail components will help to minimize wheel/ rail maintenance costs, improve safety and life-cycle matters.

According to wheel data measurements of AALRT in 2016, the wheel diameter is reduced from 660mm to 656.8mm and the flange thickness is reduced from 21.21mm to 16.36mm.

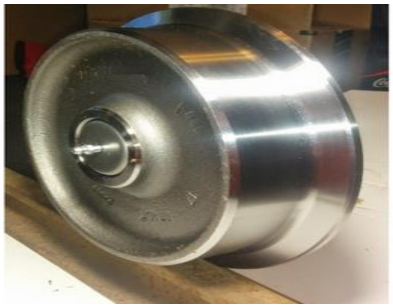

Figure 1.Wheel of AALRT vehicle

1.3. Objectives

1.3.1. General Objective

Analyzing wear resistances of wheel-rail contact surface materials in the case of AALRT.

1.3.2. Specific Objectives

- To study wear resistance of the wheel-rail material (Mn-steel and Pearlite steel)
- Model wheel and rail components using SIMPACK software
- Generating creep forces and creepages using SIMPACK software
- Determine the wear number, wear volume, specific volume of material removed, wear rate and the wear resistance of materials
- Compare Manganese steel and Pearlite steel materials based on wear and wear resistance results.

1.4. Scope and Limitations of the Study

1.4.1. Scope of the Study

This thesis is focused on studying wear resistance of wheel-rail wear materials by using collected data, studying about the wheel-rail contact materials, modeling wheel-rail pair of a train using SIMPACK software and wheel-rail wear is analyzed through numerical and analytical methods.

1.4.2. Limitations of the Study

An important consideration that has supposed to be addressed but not considered in this work is:

- Laboratory tests of wear of wheel/rail materials are not possible to perform due to absence of wear test machines like pin on disk wear test machines.
- Effect of temperature, wind, aerodynamics and vertical elevation or gradient resistance force are not considered in the current study but they influence on wheel/rail vehicle dynamics and it is another engineering problem which needs to be studied.

1.5. Significance of the Research

This study helps to identify the problems that are resulted from rolling/sliding wear of wheel/rail and analyzing the wear resistance of materials for Addis Ababa Light Rail Transit. These will also help for Ethiopian Railway Corporation to promote safety issues that are related to wear of wheel and rail components. Furthermore, this thesis contributes to decrease the number of incidents related to this component failure, increasing life time of wheel and to reduce maintenance costs. In addition, it is also a supporting document for a research on the title. Therefore, it will help as a reference for further study in the area of the above mentioned title. So as it will be a good guide for further researches.

1.6. Organization of the Paper

This thesis consists of five chapters. The first chapter is introduction and deals about background of the study, statement of the problem, objectives, scope and limitations, organization of the paper and significance of the study. While the second chapter provides a review of literatures related to this paper. The third chapter deals about analytical methods and conditions. Results and discussions are discussed in the fourth chapter. Finally, the fifth chapter deals about conclusion, recommendation and future work related to this study.

CHAPTER TWO: LITERATURE REVIEW

2.1. Wheel-Rail Contact Surface of the Railway System

The contacting bodies of the railway wheel-rail system are in continuous rolling motion [3]. In the contact zone between railway wheel and rail; the surfaces and bulk material must be strong enough to resist the normal (vertical) forces introduced by heavy loads and the dynamic response induced by track and wheel irregularities. The tangential forces in the contact zone must be low enough to allow moving heavy loads with little resistance, at the same time the normal loads must be high enough to provide traction, braking and steering of the trains. The contact zone (roughly 1 cm^2) between a railway wheel and rail which is small compared with their overall dimensions and its shape depends not only on the rail and wheel geometry but also on how the wheel meets the rail influence, i.e. lateral position and angle of wheel relative to the rail. So the small contact area needs to transfer a very high axle load, causing very high contact pressure [12].

Wheel-rail contact is a critical issue with respect to safe transportation by reducing vibration and noise sound. This phenomenon has been extensively investigated in the last decades. Since the wheel-rail contact is an open system, which is strongly influenced by wear of materials. Therefore, a great deal of research was focused on wear of materials under various contact conditions [14]. From the start, the wheel-rail contact has been of crucial interest to railway engineers. In fact, the mere idea of reducing the traction interface to a small area by using harder materials such as steel is at the core of what separates the railway from road transport [15]. The contact zone must be small compared with the overall dimensions and its shape of the wheel and rail. The contact zone size and shape in the wheel and rail contact has been estimated from the Hertz theory of elliptical contact [16].

Now a day, there is a high demand of railway transportation systems in Ethiopia for a short and long distance transport of passengers and goods. The new rail network in Ethiopia and the railway track must show the necessity of an efficient management of railway systems. The design must aim toward reducing costs and increasing safety, as well as reliability of the railway systems. The wheel/rail interface is one of the most crucial points that must be checked to determine the performance of a train and consider its safety. After having a built up of trains with a relevant rail track systems, there is a periodic maintenance schedule. Due to the applications of different load cycles, relative rolling/sliding motion of wheels on rail tracks, inappropriate geometrical fitness of wheel/rail contact profile and some other factors the maintenance schedule mainly concerns about the wheel/rail interaction systems. The contact between wheel and rail is the basic constitutive element of railway vehicle dynamics.

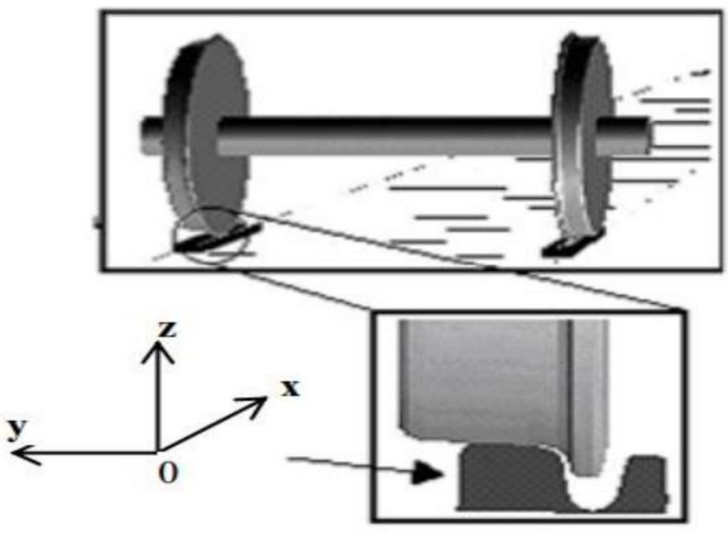

Figure 2.Rail, wheel and contact frames [17]

Since wheel–rail contact is always a hot topic for railway vehicle dynamics researchers and wheel–track maintenance engineers. Contact is the principal method of applying loads between deformable solids, and therefore is present in a wide variety of mechanical components. In addition, contacts usually act as stress concentrations, and are thus probable locations for mechanical failure. Contact stresses developed during the pressing action of two bodies' needs careful attention. Since occurrences of such forces are very frequent. Gears, Ball-and-Roller bearings, wheel on rails etc. are familiar examples. Considering the gears, ball & roller bearings, when two bodies with curved surfaces come into contact without any pressure or forces between them, the geometry of contact is in general either a point or a line. But in the case of rail - wheel system, the contact area between rail and wheel is elliptical. The contact elliptical area is small so stresses developed will be higher. For the simplest model to calculate the stresses, one uses the Hertz Theory and evaluates the effect of the weight only. The theory governing the wheel/rail contact is Hertz theory. This theory describes the fact that when two solid materials are compressed to each other by vertical loads, their contact area is formed [18].

2.2. Damage Mechanisms of Wheel and Rail Components

Damage mechanisms such as wear and plastic deformation are the main contributors to profile change. The profile change of rails on curves makes a large contribution to track maintenance cost. And the profile change on wheels can also be significant, especially on a curved track. In Europe, there are more than one hundred broken rails each year due to rolling contact fatigue. In 1995, rail maintenance costs within the European Union were estimated to 300 million Euros annually [12].

Excessive wear can affect the dynamic behavior of the railway vehicle and reduce ride comfort; impact upon the potential for derailment and reduce the integrity of the wheel material. The rolling contact of a wheel on a rail is the basis of many rail-wheel related problems including the rail corrugation, wear, plastic deformation, thermo-elastic-plastic behavior in contact, fracture, creep and vehicle dynamics vibration. Therefore, it has attracted a lot of researchers to various railway networks [22].

Rolling contact between wheel and rail can be affected by factors such as type of materials, train speed, loading, wheel/rail profiles and the reaction of the track components. Due to rapid developments in technology the performance of railway vehicles has improved significantly [24]. Assessment of contact stresses at the wheel-rail interface poses a very important issue in a study of rail-wheel contact phenomena. It is important to understand here that rail-wheel contact pair‘s profile radii change with time and wear. The way steel wheel meets the steel rail and size of the forces transmitted into contact zone influence various damage mechanisms like, wear and surface cracking. The wheel load is transmitted to the rail through a tiny contact area under high contact stress. This results in repeated loading above the elastic limit which leads to plastic deformation. The depth of plastic flow depends on the hardness of the rail and the severity of the curves [25]. The parameters that affect wear are loads, speed, time, temperature, contact type, type of environment and so on [26].

2.3. Rolling/Sliding Wear of Wheel-Rail Contact Surface Interaction

The life of railway wheels is usually limited by wear. The removal of material from the surface by wear is a function of the sliding and contact stresses. The wheel surface is subjected to high normal and tangential contact stress. Contact forces change magnitude and orientation as the wheel travels over the rail curves, crossings, and local surface perturbations. This constantly changing contact patch moves over the wheel tread and to a certain extent the flange. The wheel-rail contact is nominally rolling but a small amount of local sliding takes place at the interface. The amount of sliding depends on the contact patch geometry, normal force, lateral force and friction coefficient [5].

In the wheel–rail contact, rolling and sliding appear simultaneously in the contact zone. In curves, the wheel flange may be in contact with the gauge corner of the rail, resulting in a large sliding motion. The contact zone can be divided into two regions: stick region (no relative sliding) and slip region [27]. Sliding or rolling wear do not specify any wear mechanisms, but refer to the types of contact between two surfaces in relative motion. Instead numerous types of material removal mechanisms may appear in these types of contacts. Surface damages or wear based on adhesion or on surface fatigue are common, but also grooving by surface asperities, i.e., abrasion, tribochemical wear types and other mechanisms are possible. Nevertheless, wear and friction in sliding and rolling contacts are naturally of great interest because of their common occurrence in many machine elements. Therefore, numerous tests for sliding and rolling wear evaluations have been produced [28].

Wear is one of the common destructive phenomena which generally affect the performance and lifetime of wheel-rail contact surfaces [29]. The likelihood of railway wheel wear occurring is rising; this is as a result of new specifications imposed on railway wheels that are leading to an increase in the severity of the wheel/rail contact conditions. It is important that the wheel wear process can be modeled, as this enables improvements to be made to wheel design and materials in order to keep wear at a minimum. Excessive wear needs to be avoided as this can affect the dynamic behavior of the railway vehicles, which will reduce the ride comfort, augment the cost for maintenance and replacement of wheels, increase the vehicle-track interaction forces that may have an impact upon the potential for derailment, and reduce the integrity of the wheel material [30].

Although wear appears in the title of the conference series, there has been relatively little said about the subject. Gage face wear of rails and flange and tread wear of wheels are still important economic issues. Even with the most diligent attention not all rails in curved track are lubricated effectively all of the time. While rail head height loss by wear has become less of an issue for railroads that grind aggressively, not all railroads grind this way, and wheel treads still hollow out. There is a case to be made for a serious study of head tread wear, purely on economic grounds, but much of the recent work on wear has focused on the rail gage face. Different approaches have been taken to develop insight into the wear of wheels and rails. Reiner and Staplin observe that their equation predicts exponential increases in rail wear for wheel loads above 23 000 lbf. This stems from the adoption of an equation for rolling contact fatigue life of ball bearings as a function of load as their relation between wear life and wheel load [31].

Figure 3.Wheel / rail contact [32]

The contact between the wheel and rail of railway vehicle causes damage on the wheel threads, flange and the surface of the rails. One point to note here is that the wheels are always in contact with the rail but the rail is free of contact once the vehicle passes. Due to this, the wheels become worn out before the rails [33].

All wear rate ranges can be subdivided into three wear rate region:

- W<10e-^{6} mm rev^{-1} normal (mild);
- 10^{-6}<W<10-$^{-4}$ mm rev^{-1} inadmissible (severe);
- W>10^{-4}mm rev^{-1} catastrophic. These regions coincide approximately with the three wear regimes that are distinguished on wear-pressure or wear-slippage curves due to wear transitions [34].

Traditionally, the wear of materials has been characterized by weight loss and wear rate. However, Studies have found that wear coefficient is more suitable. The reason is that it takes to account the wear rate, the applied load and the hardness of the wear pin into. A wear volume versus distance curve can be divided into at least two regimes, the transient wear regime and the steady-state wear regime. The volume or weight loss is initially curvilinear. The wear rate per unit sliding distance in the transient wear regime decreases until it has reached a constant value in the steady-state wear regime. Hence the standard wear coefficient (K) value obtained from a volume loss versus distance curve is a function of the sliding distance [41].

Table 1.K values for various materials

Materials	K
Mild steel (on mild steel)	7×10−3
α- / β-brass	6×10−4
PTFE	2.5×10−5
Copper-beryllium	3.7×10−5
Hard tool steel	1.3×10−4
Ferritic stainless steel	1.7×10−5
Polythene	1.3×10−7
PMMA	7×10−6

2.4. Wheel and Rail Materials

Material selection for wheel/rail application is a major decision in wheel/rail analysis. In addition to the economical factor, a successful selection must take in consideration of the interaction between the track geometry, the material parameters, the environment and the service conditions. Despite the facts that wear resistance is the most significant material property for rail application.

It is difficult to obtain a material which can satisfy all the ultimate requirements including cost. However, it remains possible to achieve an optimum balance between properties and cost.

Rail steels are usually classified into three types, based on their tensile strength. These types are:

a. Normal grades: with a minimum tensile strength of about 700 MPa. Typical examples of these grades are BSll: 1978 and UIC 860-0 Grade 70. The normal grades are those used in normal service conditions in many railways. The majority of British Rail tracks and London underground is laid in BS ll Normal Grade. The chemical composition of these grades is 0.4-0.6% C, 0.05-0.35% Si, and 0.8-1.25% Mn.

b. Wear-resistant grades: with a tensile strength of about 880 MPa. These grades are characterised by hardness higher than that of the normal grades. This is achieved by refining the interlamellar spacing through increasing the carbon and manganese content. Typical examples of these grades are BS ll Wear-Resisting Grade A and BS ll Wear Resisting Grade B. Both have the same tensile strength, 880 MPa. However, BS ll Wear Resisting Grade B is harder since it contains higher percentage of manganese, 1.3-1.7%, and as a result, a refined pearlite lamellae. The wear resistant grades are used for heavy haul railway routes and in tightly curved tracks.

c. High-strength grades: with a minimum tensile strength of 1080 MPa. For very high axle loads and extremely tight curved track, higher tensile strength and further refinement of the pearlitic structure is needed. Most steel makers produced such steel by adding 1% Cr to the basic C-Mn composition. Addition of chromium increases, significantly the rail hardness and the wear resistance. Under conditions of extremely high wear rate, a very high manganese steel, around 12% Mn, can be used for high wear resistance, the mechanical properties of such steel are characterised by a high tensile to yield strength ratio. That means its work hardening rate is very high such that its hardness is almost doubled, to an appreciable depth, after a short period in service. This type of steel is used in points, crossings and other locations where the extended life can justify its cost compared with other steels [3].

According to history of wheel materials in Japan "The higher the carbon content, the higher the wear resistance. It was estimated that increase in carbon content would be effective to give the wheel a longer life."

Table 2.Steel grades specified by EN, AAR and JIS.

Region	Specification	Steel grade		Carbon content (%)	Hardness (HB)
Europe	EN 13262	ER6		≤ 0.48	234-270
		ER7		≤ 0.52	247-282
		ER8		≤ 0.56	258-296
		ER9		≤ 0.60	300-350
North America	AAR M-107/M-208	Class L		≤ 0.47	197-277
		Class A		0.47-0.57	255-321
		Class B		0.57-0.67	302-341
		Class C		0.67-0.77	321-363
		Class D			341-415
Japan	JIS E 5402-1	SSW	QS	0.60-0.75	346-407
			QR		311-363
			QRH		295-347

Dr. Saito et al. also concluded that higher carbon content of wheel material does not have any harmful influence on rail wear. Since, according to the steel grades specified by EN, AAR and JIS in Table 2, the wheel and rail materials of AALRT have similar property with ER8 steel grades. To reduce problems on wheel-rail contact, it is better to analyze and understand the wheel/rail contact material behavior and applied load conditions. The analysis of wheel/rail contact requires the detail analysis of the contacting surface conditions and factors affecting the contacting surface behavior of wheel and rail components.

On the figure below (fig.4) Wear of wheel/rail Vs carbon contents are shown. Since, on this chart if the carbon contents of wheel is decreased, there is high amount of wear on wheel. This justify that increasing the carbon contents of wheel will reduce wear of wheel material.

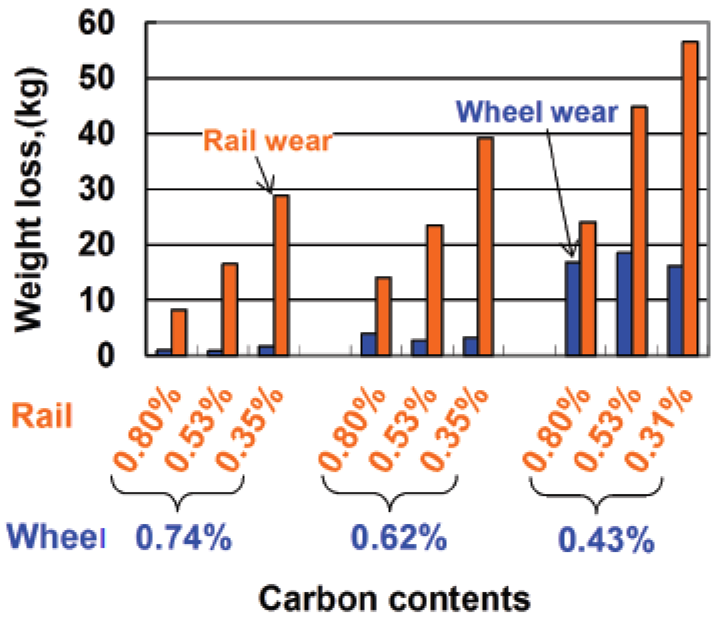

Figure 4.Wear of wheel/rail Vs carbon contents [23].

CHAPTER THREE: ANALYTICAL METHODS AND CONDITIONS

3.1. Material

It has been shown in chapter 2 that the wheel and rail materials of AALRT have similar property with ER8 steel grades. This may justify why this research has focused on ER8 rail/wheel steels. Different literatures revealed that there are several wheel and rail material standards but closely similar in their properties. In the entire standards wheel steel material is a little softer than that of the rail differing slightly in the amounts of carbon, silica, and manganese in the steels used. For Addis Ababa light rail transit (AALRT), the rail and wheel standard used is China National Railways standard which is 50 kg/m for the rail standard and 60kg/m for the wheel standard. These means that the weight of materials per unit length. The chemical composition and hardness properties of the wheel materials are tested in Akaki Basic Metals Industry (ABMI) and the rail materials are tested in Hibret Manufacturing and Machine Building Industry (HMMBI). The chemical compositions of wheel and rail materials are tested by using an equipment of SPECTROMETER with model of SPECTROTEST TXC25. This spectrometer measures the amount of elements exist in wheel/rail materials in percent. This is an advanced machine with computerized system and the working principle is by using the buttons and the system is restarted then waited until the spectrometer is refreshing. And hardness of wheel/rail materials is tested by using BRINELL HARDNESS TESTING machine which is an Italian equipment with model of 206RT. This machine tests the hardness of materials using the method of BHN parameter and it is commonly used simple and inexpensive method. The hardness test can be used in all materials, from soft to hard ones and even for carbides. It can be also used both for micro- and macro hardness where a sample is placed in the machine and indenter is pushed with a certain load against the surface of the sample. The piece of materials to be tested is prepared from Ethiopian Railway Corporation (ERC).

- Procedures for chemical composition test:
    - Wheel/rail piece of materials were prepared
    - Polish the specimen in order to have smooth surface finish and remove impurities
    - Placing the test piece on bench by pressing the on button until the whole chemical composition is displayed.
    - Conduct chemical composition test 3 times

- Take average of the tested results

- Procedures for hardness test:
  - Prepare piece of materials
  - Place a sample in the machine
  - Push an indenter with a certain load against the surface of the sample
  - Conduct hardness test 3 times
  - Take average results

The chemical composition, hardness and mechanical properties of these materials are presented below which is summarized from Appendix A.

Table 3.Chemical composition and hardness of material A and material B

Materials	Type of Structure	Specification		Chemical Composition (%)						Hardness (BHN)
				C	Si	Mn	P	S	Cr	
Material A (Mn-Steel)	Banaitic	EN13262	Wheel	0.50	0.28	0.8	<0.05	<0.05	-	275
			Rail	0.60	0.35	1.20	<0.05	<0.05	-	290
Material B (Pearlite Steel)	Pearlitic	AAR-M107	Wheel	0.70	0.35	1.25	-	-	0-0.3	321-363
			Rail	0.83	0.95	1.45	-	-	0-0.5	341-415

Table 4.Mechanical Properties of Steels of material A and material B

Materials		Tensile strength (MPa)	E (GPa)	Density Kg/m3	Poisson's ratio
Material A	Wheel	500	210	7800	0.30
	Rail	540	207	7800	0.30
Material B	Wheel	855	210	7870	0.3-0.5
	Rail	880	206	7870	0.3-0.5

3.2. Dimension

- The principal rolling radii of the wheel: R_{1w} = 330 mm
- The principal transverse radii of the wheel: $R_{2w} = \infty$
- The principal rolling radii of the rail: $R_{1r} = \infty$
- The principal transverse radii of the rail: R_{2r} = 300 mm

- Axle radius = 90 mm

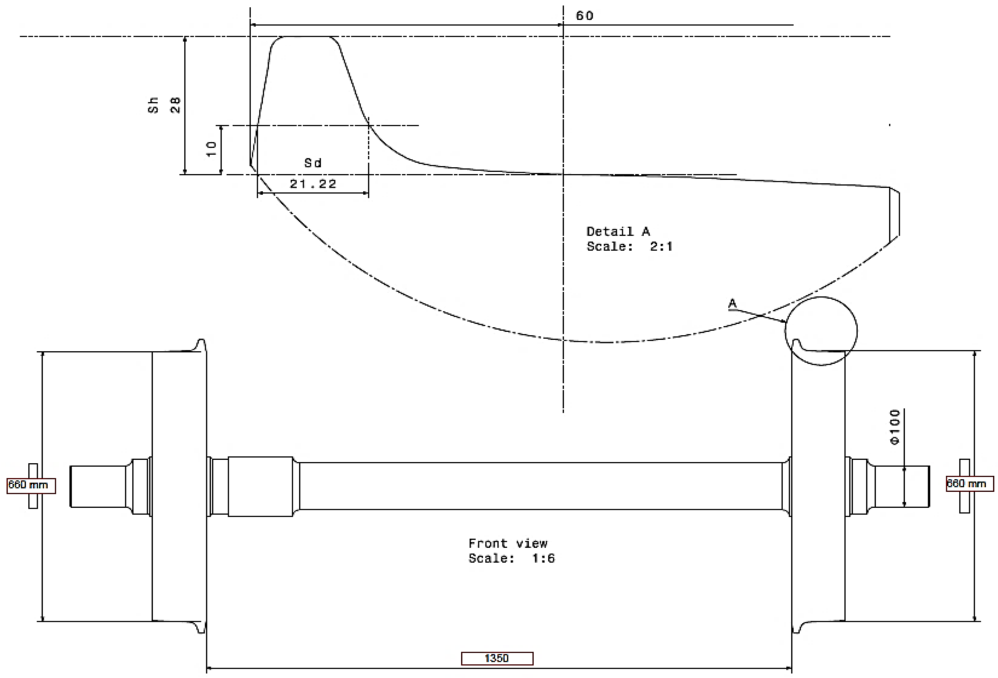

Figure 5.Standard wheel dimensions

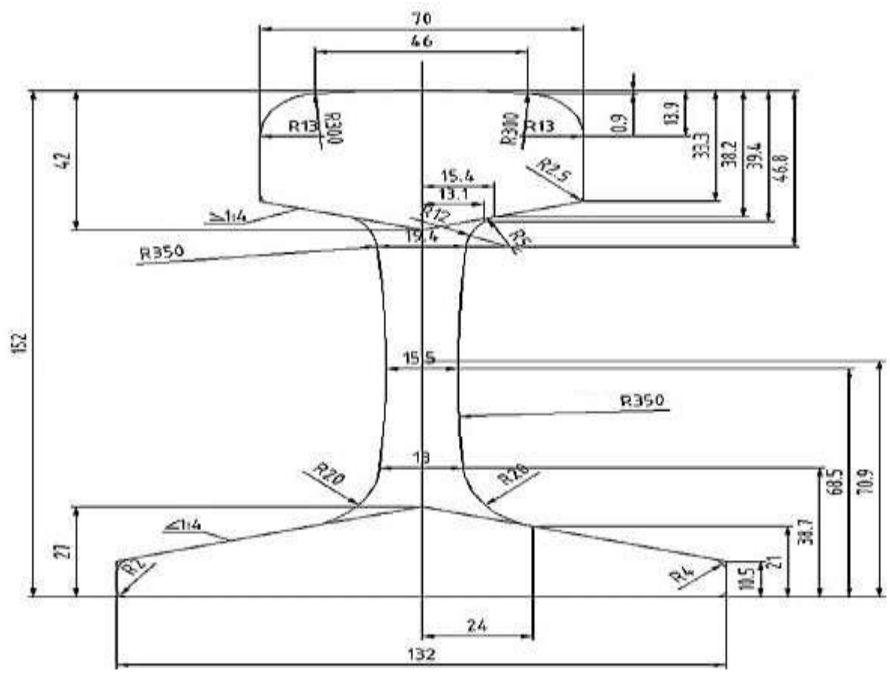

Figure 6.Standard rail dimensions [42]

3.3. Method

This thesis is done on the specific area of AALRT and most of the data is collected from Ethiopian Railway Corporation. In addition to this Metals and Engineering Corporation (METEC) also helps me testing chemical composition and hardness of wheel and rail materials using spectrometer and hardness tester machine. The life of railway wheels is usually limited by wear. To identify the causes that led to wear of wheel at AALRT, wide range of combined factors are possible and in order to identify these causes, data collection is carried out through oral interviews, reading maintenance manuals, visual inspections of track and vehicle components. The purpose of this thesis is analysis of wear and wear resistance of wheel/rail contact surface materials using numerical and analytical methods.

3.3.1. Wheel Inspection of AALRT Vehicles and Previous Results

Actual wheel data measurements were undertaken at both depots of Kaliti and Ayat by AALRT technicians and availability of data records from February 2016 to December 2016 which are helpful for wheel/rail investigation. The inspection of vehicles and track is carried out for the purpose of examining and measuring vehicle wheel and rail conditions. This inspection helps to investigate the wheel/rail conditions. Full measurements of wheel flange thickness and tread diameter were taken before and after machining of the wheels. A total of 24 vehicles operating from both depots, which were inspected the time frame as mentioned earlier. 9 vehicles inspected at Ayat depot while 15 vehicles inspected at Kaliti. The vehicle number is given by Ethiopian Railway Corporation to know loss of wheel diameter and flange thickness for each vehicle. Previous data records of the wheel inspection of Kaliti depot is shown below. Table 5 shows the summary of vehicles that were inspected at the Kaliti depot.

Table 5.AALRT Vehicles inspected between February 2016 and December 2016.

Vehicle Number	Depot Location
205, 206, 207, 208, 209, 210, 211, 212, 213, 215, 216, 217, 218, 219, 220	Kaliti wheel re-profiling workshop

3.3.2. AALRT vehicles of North-South Line (Kaliti Depot)

In this investigation, wheel data measurements of AALRT vehicles from Kaliti route, which were recorded by AALRT workshop personnel. Vehicles traveled some mileages were taken before wheel-lathe machining at their respective depot. The purpose of the analysis is to find out the amount of loss of mass affected due to wear. Table 6 shows vehicles from Kaliti route, used for comparison of flange thickness and tread diameter which are selected based on total average mileage run similarity.

- New wheel diameter 660mm, worn limit 580mm
- New flange thickness 21.21mm, worn limit of 15 mm

Table 6.Vehicles selected with mileage run

North-South Vehicle No.	Mileage run [km]
212	44,026
205	49,030
215	37,312
208	43,452
218	54,471
206	75,028
216	66,522
210	51,662
Average run [km]	53,937.88

The following two tables show flange thickness (S_d) and thread diameter (T_d) of vehicles from Kaliti routes summarized from Appendix B.

Table 7.North-South (Kaliti) vehicles Flange thickness (S_d)

Vehicle No.	**Flange thickness (S_d) in mm for respective wheels**											
	1		2		3		4		5		6	
	L	R	L	R	L	R	L	R	L	R	L	R
212	16.06	17.5	17.02	13.66	16.49	17.69	17.48	17.62	16.63	19.38	16.41	16.93
205	16.71	16.54	17.48	13.48	17.38	18.24	16.38	17.37	16.48	16.59	17.59	18.51
215	17.07	17.93	15.46	13.46	18.05	16.75	17.09	15.45	16.54	16.65	16.17	16.03
208	16.34	17.53	13.45	18.34	17.05	15.44	17.28	14.47	18.68	16.96	17.09	15.99

218	13.70	16.65	14.16	13.86	17.08	16.14	14.11	12.83	18.38	18.06	16.02	15.26
206	17.08	16.77	16.57	15.74	15.41	15.38	14.60	14.34	16.52	16.09	16.07	15.47
216	16.52	16.10	15.96	15.02	17.86	16.84	18.15	17.53	18.47	16.75	16.60	14.75
210	16.12	16.36	16.30	14.39	15.52	14.21	17.51	17.45	16.40	16.93	16.38	14.98
Average S_d/wheel	**16.20**	**16.92**	**15.80**	**14.74**	**16.86**	**16.34**	**16.58**	**15.88**	**17.26**	**17.18**	**16.54**	**15.99**
Average S_d/bogie	**15.92**				**16.41**				**16.74**			

Note: L – left wheel, R – right wheel

*Total average flange thickness of Kaliti vehicles = 16.36 mm

- Total loss = New wheel – Worn wheel = 21.21- 16.36 = 4.85mm,
- Percentage loss = (4.85/21.21)*100 = 22.9 %

As shown in the above, the average flange thickness per wheel of Kaliti vehicles is greatly worn, with an average flange thickness of 16.36 mm and a total percentage loss of 22.9 % in flange thickness. One of the reasons to loss of this flange thickness is due to wear of wheel materials. Since there exists so many number of contacts between wheel and rail during transportation. Different literatures show that there are at least ten billion contacts per year between wheel and rail components. During such contacts wear will be created on wheel and rail components. This is especially due to adverse conditions of sharper curves in the route. The following table 8 also shows tread diameters of vehicles. The average tread diameters per wheel and per bogie are computed for vehicles.

Table 8.North-South (Kaliti) vehicles Tread diameter (T_d)

Vehicle No.	**Tread diameter (T_d) in mm for respective wheels**											
	1		2		3		4		5		6	
	L	R	L	R	L	R	L	R	L	R	L	R
212	659.7	659.6	659.7	659.4	660.1	660.1	660.1	660.2	659.3	659.9	659.6	659.5
205	659.4	659.5	659.6	659.6	660.2	660.2	660.0	660.0	659.6	659.6	659.6	659.7
215	659.6	660.0	659.8	659.7	660.3	660.4	660.1	660.3	659.8	659.8	659.8	659.8
208	659.4	659.5	659.6	659.8	660.1	660.3	660.2	660.1	659.7	659.6	659.4	659.6
218	659.3	659.6	659.3	659.4	660.2	660.2	659.9	659.9	659.1	659.7	658.9	659.3

206	648.5	648.5	647.4	647.5	638.8	638.9	637.3	637.6	652.6	652.7	652.4	652.6
216	648.9	649.1	645.6	645.5	660.0	660.0	660.0	659.8	647.3	647.2	647.2	647.3
210	659.0	659.3	659.4	659.2	660.1	660.3	650.7	650.9	659.3	659.5	659.2	659.2
Average T_d/wheel	**656.7**	**656.9**	**656.3**	**656.3**	**657.5**	**657.6**	**656.1**	**656.1**	**657.1**	**657.2**	**657.0**	**657.1**
Average T_d/bogie	**656.5**				**656.8**				**657.1**			

*Total average tread diameter of Kaliti vehicles = 656.8 mm

- Total loss = New wheel – Worn wheel = 660 – 656.82 = 3.19 mm,
- Percentage loss = 0.48 %

As shown in the above, average tread diameter per wheel of Kaliti vehicles is greatly worn, with average tread diameter of 656.8 mm with a total percentage loss of 0.48 % in tread diameter. Therefore, there is loss of mass in the wheel components as shown from the above two tables.

3.3.3. Seating capacity of AALT vehicles

The vehicle is designed to hold many passengers at a time and designed for more people to stand to use space for servicing at once.

Table 9.Seating capacity of AALRT vehicle

Number of passengers (persons)	Seated	Standing	Total
Seats (AW1)	65	0	65
Seating capacity (AW2) (standing: 6 persons/m2)	65	189	254
Overload capacity (AW3) (standing: 8 persons/m2)	65	252	317

3.3.4. AALRT Vehicle weight

Weights of vehicles are given in the following table with vehicle axle load and taking 60 kg as average weight of each passenger.

Table 10.Vehicle weight of AALRT

Loads	Vehicle body weight	Passenger weight	Total weight
Empty vehicle (t)	44	0	44
Seating capacity (t)	44	15.24	59.24
Overload capacity (t)	44	19.02	63.02

Note: Total weight = Vehicle body weight + Passenger weight

3.3.5. Coefficient of Friction between Wheel and Rail Contact

The coefficient of friction is defined as the friction force (tangential force) divided by the normal force which loads the system. It is a dimensionless quantity and can depend on dimensionless combinations of system parameters like material properties, speed and load applied on the system. Railway technology is strongly influenced by the friction coefficient between wheel and rail. The study of the wheel/rail contact always involves the presence of friction. The wheel - rail contact is modelled in terms of contact and friction. There is friction between two bodies in contact and the coefficient of friction is determined by the type of contact on materials. In wheel-rail contact case, wheel material is a little softer than rail material. Therefore, 0.3 is preferred as a coefficient of friction in a contact of steel on hard steel as shown in the table below (table 11).

Table 11.Coefficient of friction in wheel-rail contact

Material	Condition	Average Speed (Km/h)	Load (N)	μ
Steel on hard steel	Dynamic	40	53787.3	0.30
	Static	0	>>	0.40
Soft steel on cast iron	Dynamic	40	>>	0.12
	Static	0	>>	0.17
Hard steel on cast iron	Dynamic	40	>>	0.10
	Static	0	>>	0.15

3.3.6. Forces in Wheel-Rail Contact

Vehicle dynamics performance is strongly influenced by interacting wheel and rail forces. In wheel–rail contact tangential force and normal force exists, i.e., the transmitted tangential force in the longitudinal direction during driving and braking, plays an important role in all these aspects. On the other hand the normal force in the vertical direction due to vehicle and passenger loads can exist in the wheel-rail contact surface. These Forces are directly transferred to the wheel through the axle.

a) Normal Force

The wheel is subjected to normal force, F_N, and travels along the rail at velocity v.

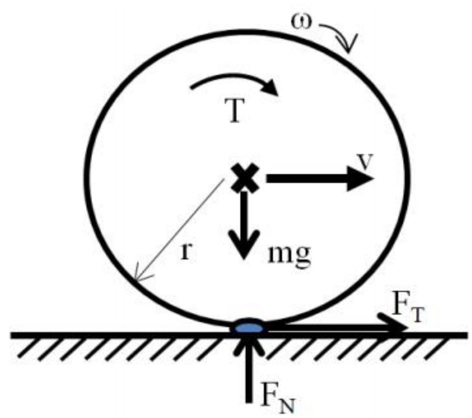

Figure 7.A rolling–sliding contact under acceleration (X is the gravity center; all forces in the figure are acting on the wheel)

As shown in Figure 7, assume a single vehicle running with acceleration a, whose load is equally distributed on the wheels, all of which are powered. The vehicle is subject to gravity, mg. F_N is the normal force and F_T is the tangential force for each wheel. The following equations can be obtained:

$$\sum F_N = mg \quad \text{……} (1)$$

where: F_N – Normal force

m – total mass,

g – gravity

Therefore, F_N = 63,020*9.81 = 618,226.2 N

Since, 618,226.2 N normal loads are distributed in all wheels of a tram. One tram contains 12 wheels. So, F_N /wheel = 618,226.2 N /12 = 51,518.85 N. It is an applied normal load on one wheel.

b) Tangential Force

As shown figure 7 the wheel is subjected to torque, T, which maintains the angular velocity of the wheel, ω, and also causes a reactive tangential force, F_T, at the wheel–rail interface. The tangential force of a driving wheel is known as traction, which ultimately propels the wheel along the rail. During deceleration, the tangential force, F_T, opposes the running direction due to the braking torque, T, applied anticlockwise. The tangential force can be obtained as:

$F_T = \mu F_N$ ……………………………………………………………………………...………… (2)

where: F_T – tangential force

μ – coefficient of friction

F_N – normal force

Therefore, F_T = 0.3*51,518.85 = 15,455.655N per wheel

c) Resultant force

The resultant force acted on wheel-rail contact is:

$F_R = \sqrt{F_N^2 + F_T^2}$ = 53787.3N………………………………………………………… (3)

3.3.7. Wheel/Rail contact

A railway vehicle consists of wheel sets, bogies, and a body, where the wheel sets and bogies are connected through primary suspension systems while the bogies are connected to the car body through the secondary suspension systems. Figure 8 shows a typical railway vehicle consisting of the mentioned components.

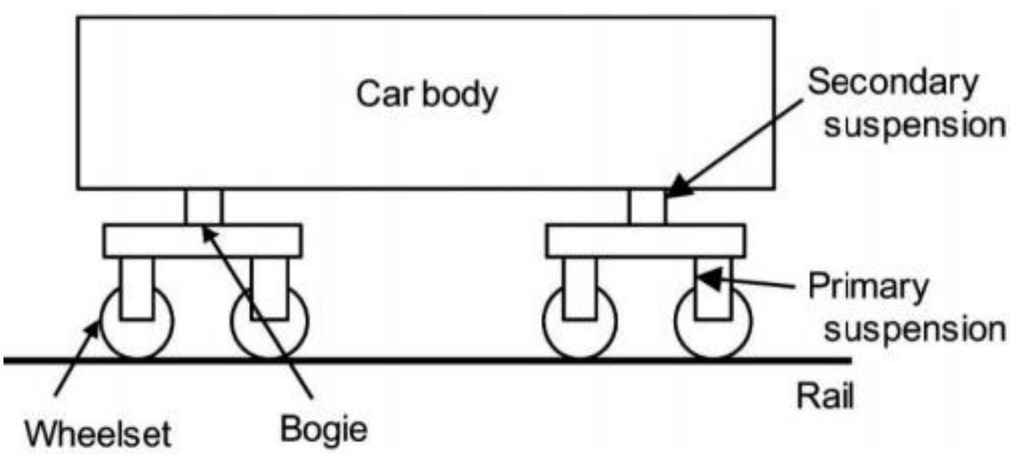

Figure 8.Configuration of railway vehicle [38]

Wheel is always in contact with rail but the rail surface may be free in some times after the wheel passes. To make clear understand about this interaction of wheel and rail materials, it is enough to see figure 9.

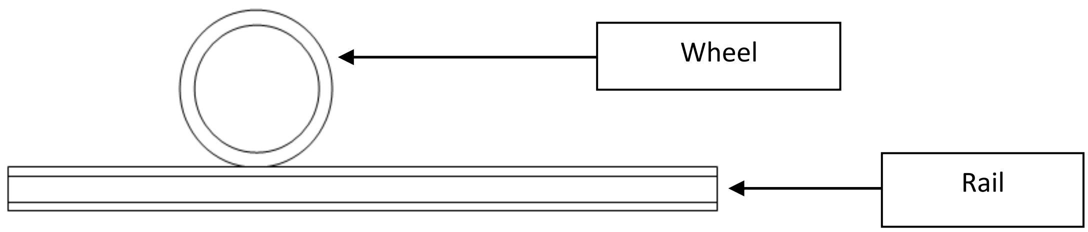

Figure 9.Contact between wheel and rail

Vehicle dynamics performance is influenced strongly by interacting wheel and rail forces.

There are two planes considered in contact forces as shown below in figure 10.

• Plane 1 (Normal plane):- This plane involves constraint forces namely the normal force and geometry forces. ‘Q’ denotes the vertical force acting on the contacting point, while ‘N’ is the normal force and ‘Fy’ denotes the lateral force.

• Plane 2 (Tangential plane):- Tangent forces or creep forces such as T_x, T_y friction forces in x, y direction, which depend on longitudinal (S_x) and lateral (S_y) creepages.

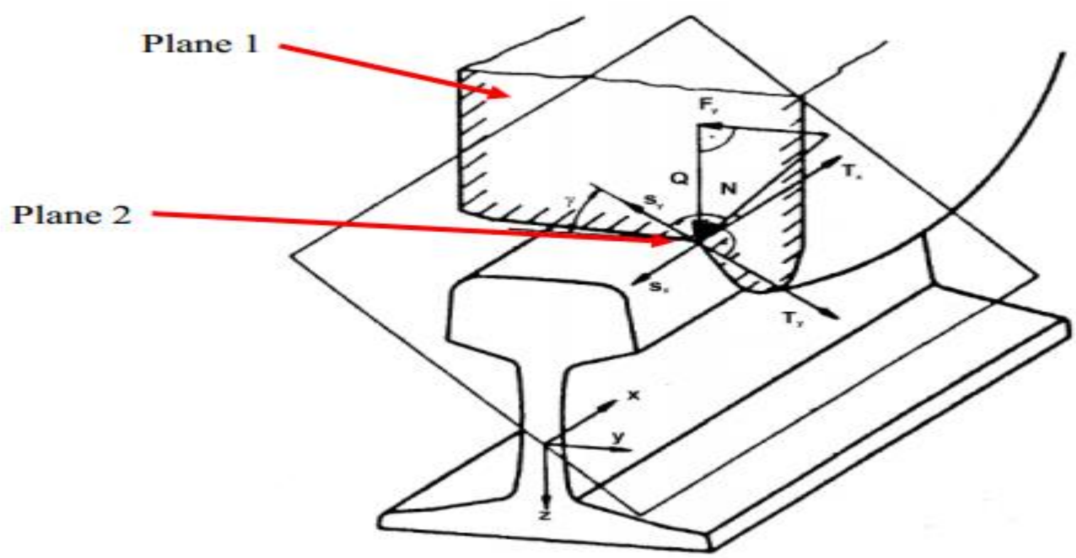

Figure 10.Wheel/rail contact forces

3.3.8. Derailment Coefficient

The derailment ratio Y/Q is used as a measure of the running safety of a railway vehicle. Several theories have been developed to establish the Y/Q ratio. One of the most widely used is the Nadal [1908] derailment criterion which describes the conditions necessary to sustain equilibrium of the forces in flange contact. Description of the Nadal theory can be found in Dukkipati [2000].

Nadal's formula takes into account the influence of the wheel flange angle, the wheel/rail friction coefficient, and wheel/rail forces on the possibility of wheel climb derailment. This principle is expressed in Nadal's formula:

$$\frac{Y}{Q} = \frac{\tan\phi - \mu}{1 + \mu\tan\phi} \dots\dots\dots\dots\dots\dots\dots\dots\dots\dots\dots\dots\dots\dots\dots\dots\dots\dots\dots\dots\dots\dots\dots\dots\dots\dots\dots\dots\dots.(24)$$

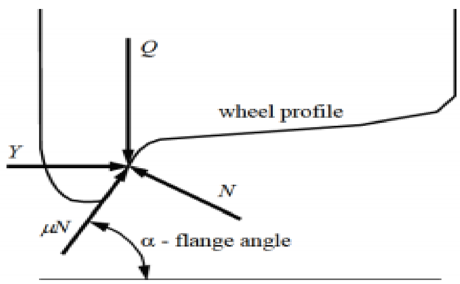

Q vertical force;
Y lateral force;
α flange angle
μ friction coefficient

Figure 11.Flange angle and flange forces [39]

3.3.9. Analysis of Wear

Wheel wear is closely related to conditions of force and slip in the wheel/rail contact. Two basic types of wear models are described in the literature on wheel/rail.

1. Sliding models where material loss depends on combinations of sliding distance, normal force, and material hardness.

- Wear volume = $K \frac{\text{distance traveled} * \text{Normal load}}{\text{hardness}} = K \frac{s * F_N}{H}$ …Archard's wear model..…..(25)
- W = f(H_W, H_r)
- Wear rate: - is defined as wear volume per distance. i.e

  Wear rate (W_r) = wear volume/Distance = W_v/s [m^3/m]……………...………...……. (26)
- Wear resistance: - is a reciprocal of wear rate. i.e R = 1/W_r …………………...…… (27)

Based on the above Archard's wear model eq. (25) the following conclusions have been achieved:

- The material volume removed by wear is proportional to the sliding distance;
- The material volume removed by wear is proportional to the normal applied load;
- The materials display a wear amount inversely proportional to their hardness.

2. Energy transfer models, which assume material loss to be a function of the energy dissipated in the contact patch. Pearce and Sherratt [1990]), have shown that the wear of wheels and rails depends on the rate of dissipation of energy within the contact patch. It had been concluded that wheel wear rate could be related to the energy expended through creepage in each wheel/rail contact. This can be shown to be the sum of the products of the individual creep forces and creepages in the longitudinal and lateral directions. Wheel wear is estimated using the wear index taken from the English Normative (British Rail) that reads [39]:

$$W = Fx \cdot \xi + Fy \cdot \eta \quad (28)$$

Where, **Fx** is the longitudinal creep force; **ξ** is the longitudinal creepage; **Fy** is the lateral creep force; **η** is the lateral creepage.

Variables such as longitudinal creep force, longitudinal creepage, lateral creep force and lateral creepage, are calculated in SIMPACK by performing time integration of the parameter variation. The wear of the wheels is greater on curves of small radius. Therefore, the wheel-rail pair simulation is done on minimum curved radius R50 m track of AALRT line with transition track of 15 m. After attaining the results of the simulation, the results are exported into excel and wear index is calculated.

3.3.10. Wheel-Rail pair modeling using SIMPACK

SIMPACK is a multi-body simulation package that is used to simulate and model complex mechanical systems. And also used to predict and optimize the behavior of any type of multi-body system by solving the equations of motion. The software allows the user to make determination of wheel-rail contact geometry, making an online and offline time integration, generating creapages and creep forces, determining wear numbers and derailment coefficients.

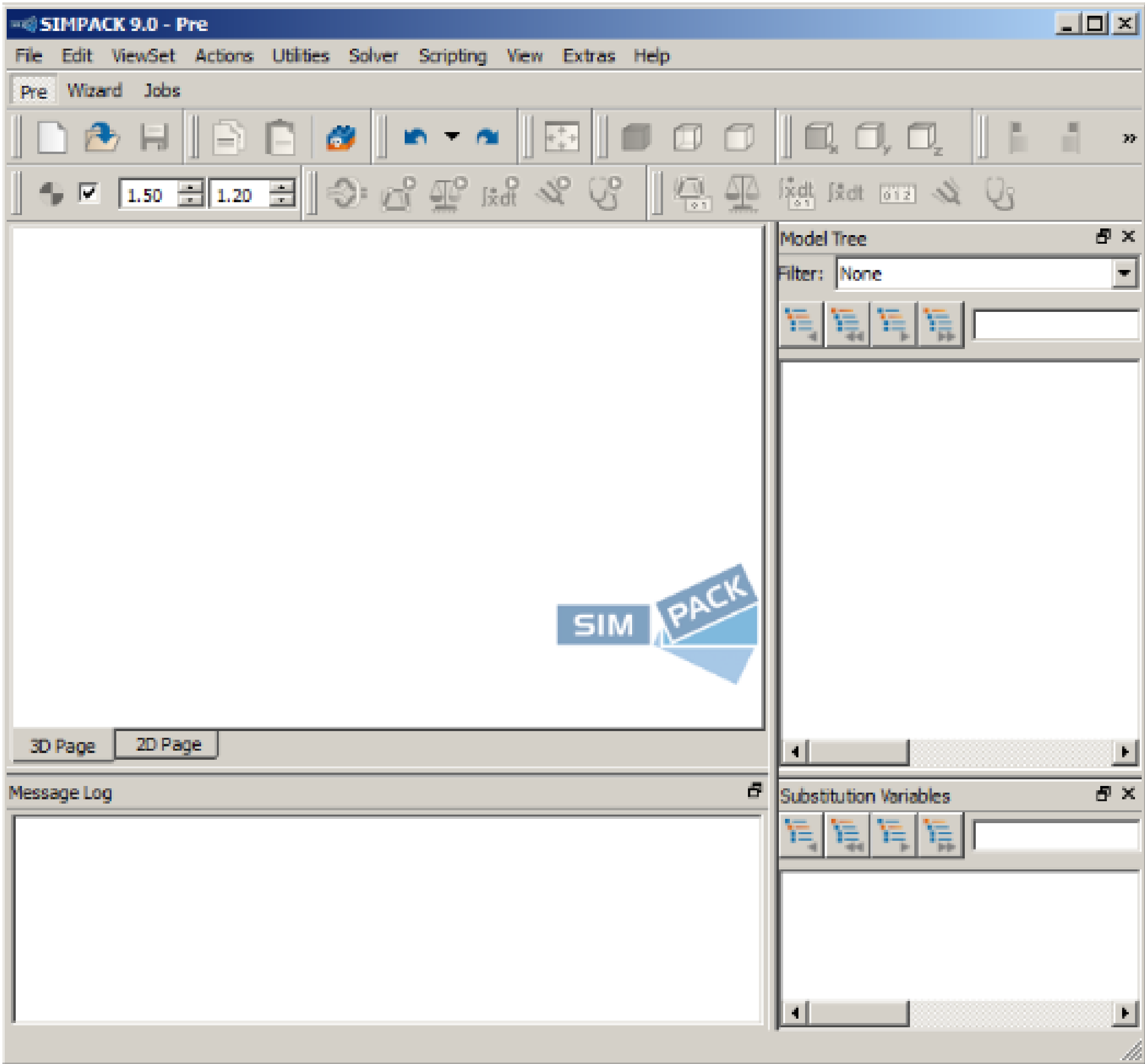

Figure 12 SIMPACK GUI Pre-Processor ViewSet

As we can see from GUI (figure 12), the SIMPACK ViewSet is divided into four areas:

- **3D/2D Page: -** it is the biggest area which is found on the left as you have seen.
- **Message Log: -** This is where important messages, such as modeling information, print outs, warnings are displayed.
- **Model Tree: -** is found on the right which lists all modeling elements of the work, you can also create new modeling elements here.
- **SubVars: -** The **SubVars** area will list all 'Substitution Variables', i.e. parameters that are defined in the model.

3.3.11 Basic Input Parameters Based on AALRT Specification

- Wheel Diameter: 660mm
- Maximum Running Speed: 80km/hr
- Maximum Operating Speed: 70Km/hr
- The maximum Axle Load: 22ton (Power bogie 10.5t + Trailer bogie 11.5t)
- Max. width of car body： 2650mm
- Car body height (to rail top)： 3025mm
- Wheel Type: S1002 with flange angle of 70^0 and flange thickness (S_d) 21.21mm
- Rail Type: UIC 60
- Track Gauge: 1435mm
- Tramcar Width: 2650mm
- Tramcar Height: 3700mm
- Minimal Curve Radius: 50m for mainline and 30m for parking garage
- Tramcar Length: 28400mm
- Wheel Base: 1900 mm for power bogie and 1600 mm for driven bogie

The general process of wheel set modeling consists of the following basic operations:

- Step 1. Setting up the wheel set model
- Step 2. Bringing the wheel set into an initial equilibrium
- Step 3. Adding a simple guidance (primary springs) to the wheel set

Input data for wheel set modeling:

- Axle diameter = 180mm
- Axle length = 2200mm
- Wheel diameter = 660mm

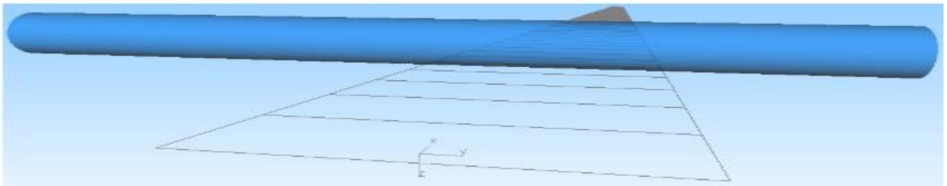

Figure 13 Wheelset shaft with Track

Based on the given input data, we can model wheel-rail pair using SIMPACK software. The Wheel-Rail Pairs are the central data container and manage all Modeling Elements related to the wheel-rail contact.

- Create the right-hand wheel-rail pair
- Create the left hand wheel-rail pair

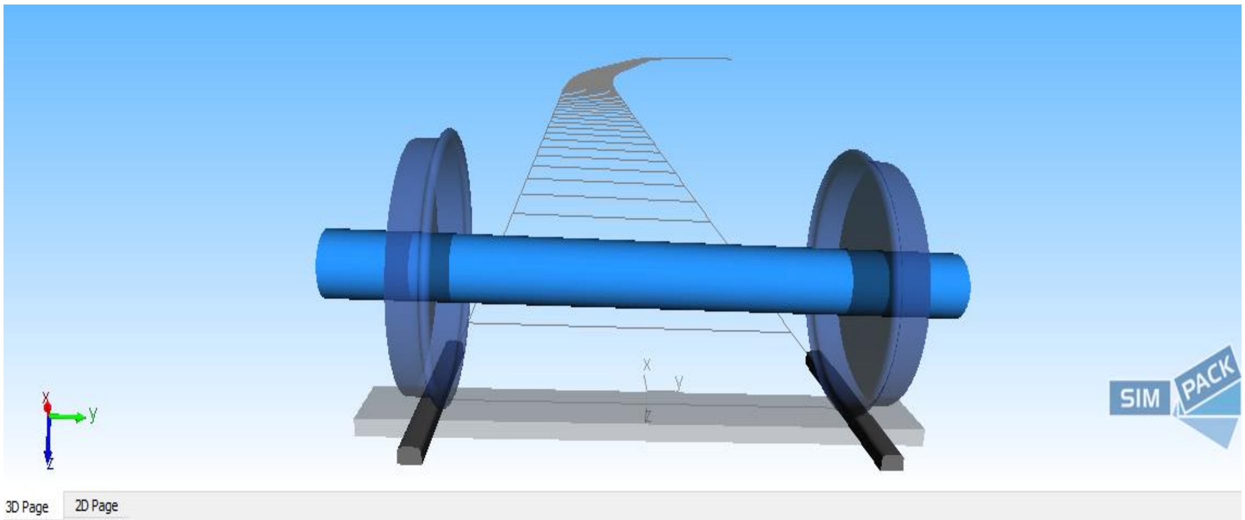

Figure 14.Wheel-rail pair model of AALRT

Figure 14 shows that wheel-rail contact model of AALRT using SIMPACK software.

a) Creepages and Creep Forces

Carter [1926] was the first to study creep in railway wheels. The relationship between creepage and creep force has been studied thoroughly by Kalker [1967, 1982 and 1990]. The wheel and the rail interface through a small contact patch. The centre of this contact patch is the application point of normal force, F_x and tangential force, F_y. The concept of creepage has been studied in the field of railway vehicle dynamics for many years and is well understood. De Pater [1962] and Johnson [1958] analysed the motion of the wheel with respect to the rail. The creep velocity divided by the rolling velocity is called correspondingly longitudinal ξ and lateral η creepage:

i.e. $\xi = \frac{V_x}{V_{roll}}$ and $\eta = \frac{V_y}{V_{roll}}$ … (29)

The forces acting in each contact area, in the contact axis system, are obtained by evaluation of the creep forces.

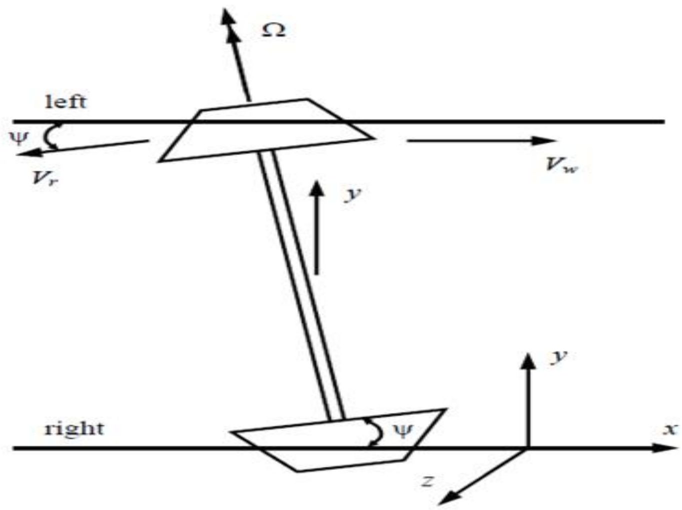

Figure 15.The creepages of wheelset on a track

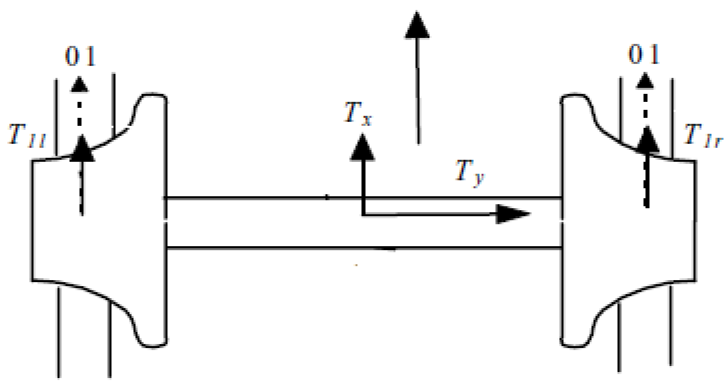

Figure 16.Creep forces in the wheelset [8]

SIMPACK software generates creepages and creep forces in SIMPACK simulation after attaining time integration. Since, the simulation is done at operating speed of 20km/h in curved tracks. For this operating speed, the longitudinal creepage, lateral creepage, longitudinal creep force and lateral creep force are obtained from the simulation as shown in Appendix C. The following diagrams (fig. 17 & 18) show the values of creepages and creep forces at curved track operating speeds respectively for Manganese steel and Pearlite steel. Based on such diagram the maximum and minimum values of creepages and creep forces are evaluated for Manganese steel and Pearlite steel.

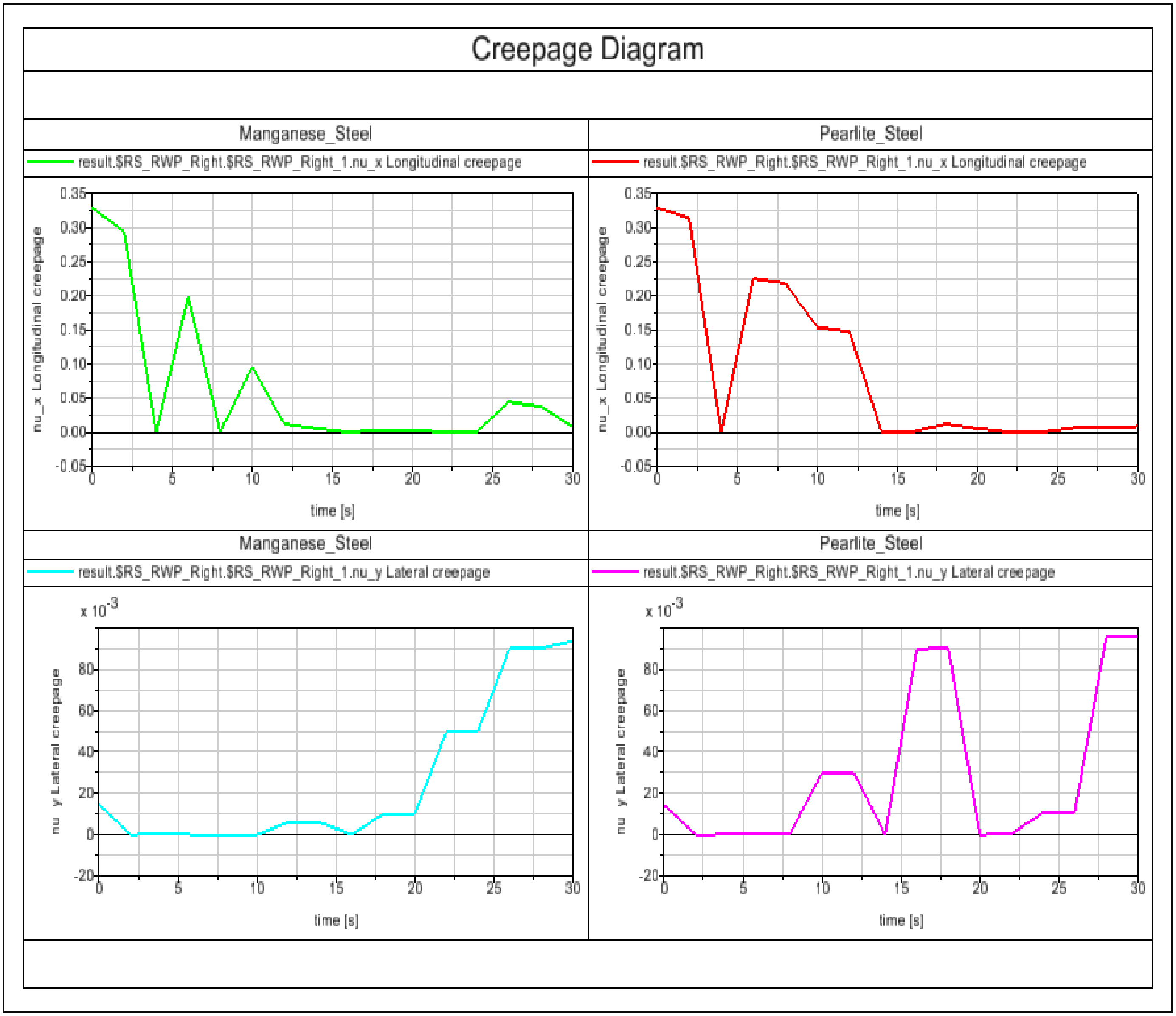

Figure 17.Longitudinal and lateral creepages at operating speed of curved track

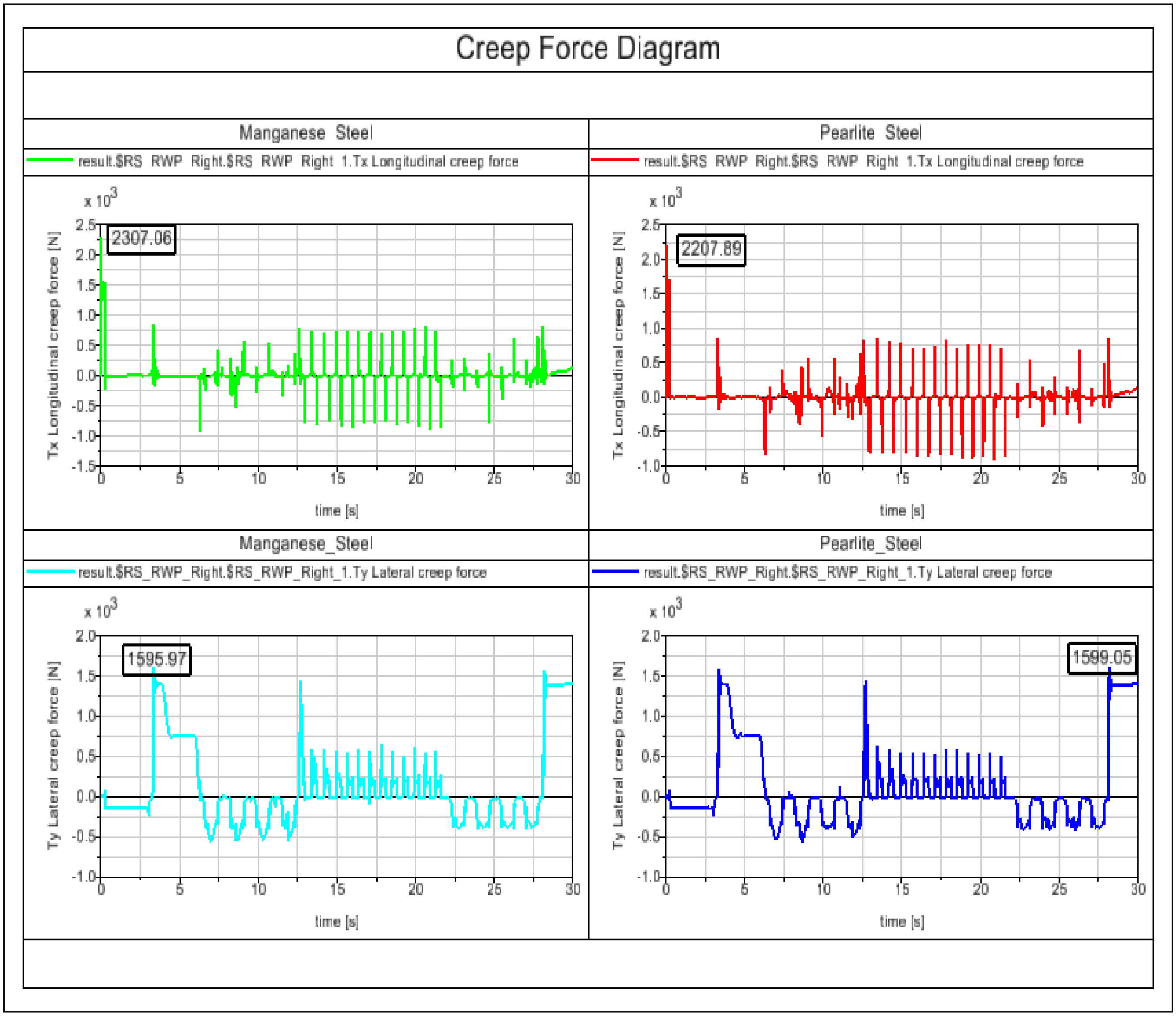

Figure 18.Longitudinal and lateral creep forces at operating speed of curved track

Figure 18 shows that diagram of Longitudinal and lateral creep forces. Since, based on these diagrams the maximum longitudinal creep force of Manganese steel and Pearlite steel are 2307.06 and 2207.89N respectively. And the maximum values of lateral creep forces are 1595.97 and 1599.05N for Manganese steel and Pearlite steel respectively.

The general values of creepages and creep forces for Manganese steel and Pearlite are tabulated as follows. These values of creepages and creep forces are generated after time integration of wheelset modeling on SIMPACK software.

Table 12.Creepages and creep forces of Mn-steel

Time [s]	Longitudinal Creepage	Lateral Creepage	Longitudinal Creep Force [N]	Lateral Creep Force [N]
0	0.329185	0.0144482	1479.51	10.0297
2	0.294144	0	285.605	0
4	0	0.000412778	0	1595.97
6	0.199003	4.61E-05	1921.2	1464.11
8	1.90E-06	1.02E-05	2307.06	1305.79
10	0.0955539	9.98E-06	983.965	1333.95
12	0.0116855	0.0060323	8.77232	18.5352
14	0.00524612	0.00581535	9.31058	32.0686
16	1.14E-07	0.000125343	9.8486	168.259
18	0.00299102	0.00983399	121.007	1397.35
20	0.0030256	0.0100129	121.581	1397.32
22	2.80E-07	0.0498172	122.155	1397.28
24	1.11E-06	0.0500604	122.729	1397.29
26	0.0439277	0.0899177	123.303	1563.34
28	0.037475	0.0902276	123.878	1397.39
30	0.00787917	0.0936588	132.525	1397.37

Table 13.Creepages and creep forces of Pearlite steel

Time [s]	Longitudinal Creepage	Lateral Creepage	Longitudinal Creep Force [N]	Lateral Creep Force [N]
0	0.329189	0.0143141	1085.19	11.8173
2	0.313952	0	339.878	0
4	0	0.00013637	0	0.118827
6	0.224961	0.000251396	1877.64	2.96158
8	0.218385	0.000660758	2207.89	13.89641
10	0.153694	0.0299601	230.545	1304.2
12	0.147224	0.0301834	385.752	1245.71
14	0.000779776	1.32E-05	1833.39	1227.13
16	0.000719857	0.0898169	34.7174	440.739
18	0.011521	0.0901307	34.9561	540.109
20	0.00508919	4.93E-06	36.3117	216.176
22	2.87E-05	0.000437663	37.2526	608.348
24	3.43E-05	0.0106067	2.1853	1138.93
26	0.00595952	0.0107728	136.337	1484.95
28	0.00601162	0.0955037	136.896	1599.05
30	0.00836782	0.0958219	137.459	1397.33

3.3.12. The wear model

The calculation of wear on the wheel is based on the volume of the removed material correlates with the total frictional work. The main output of the wear model is the specific volume $\delta P_{ki}^{j}(t)(x,y)$, expressed in $mm^3/(mm^2m)$, a function of time which describes the specific volume (the volume per unit of area and per unit of travelled distance) of the material to be removed in the grid position(x, y) of the contact patch $P_{ki}^{j}(t)$.

The integral with respect to x and y over the grid gives the specific volume of the removed material per unit of travelled distance relative to the contact patch P_{jki} (t). In fact, the subscript P_{jki} (t) indicates the contact patch i^{th} of the wheel j^{th} in the k^{th} multibody simulation of the statistical analysis of the track.

The wear rate gives a measure of the amount of material removed per meter of travelled distance (m) travelled by the train and per mm^2 of surface. The analytical expression for K_w (I_W) is given by Equation (31).

$$K_W(I_W) = \begin{cases} 5.3 * I_W, & I_W < 10.4\ N/mm^2 \\ 55.0\,, & 10.4 \ \le\ I_W\ \le 77.2\ N/mm^2 \\ 61.9 *\ I_W\ - 4723\,, & I_W\ > 77.2\ N/mm^2 \end{cases} \dots\dots\dots\dots (31)\ \ [34]$$

Normally, the wear rate on the tread is typically K1, while on the flange both the K1 and K2 regimes occur.

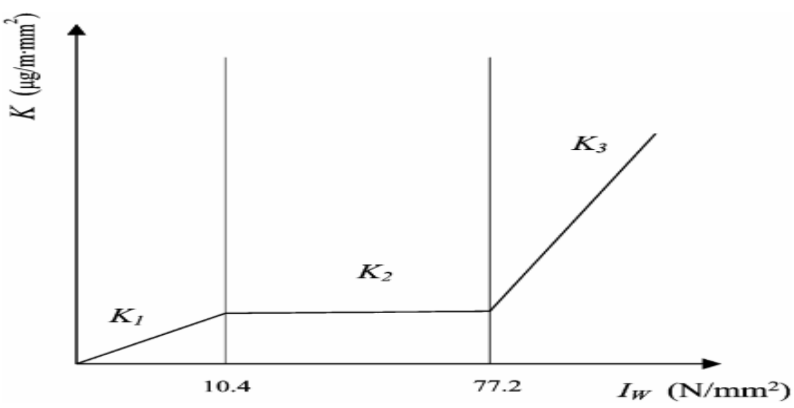

Figure 19.The wear rate as a function of wear index [40].

After evaluating the wear rate, the specific volume $\delta P_{ki}^{j}(t)(x,y)$can be calculated as follows:

$$\delta P_{ki}^{j}(t)(x,y) = \frac{K\, I_W}{\rho}\left(\frac{mm^3}{m\ mm^2}\right) \dots\dots\dots\dots\dots\dots\dots\dots\dots\dots\dots\dots\dots\dots\dots\dots\dots\dots\dots\dots (18)$$

Where, ρ is the material density of the wheel and rail (expressed in kg/m^3).

CHAPTER FOUR: RESULTS AND DISCUSSION

4.1. RESULTS

4.1.1. Wear Analysis Results

a) Determining wear of materials

Table 14.Wear volume of material A (Mn-steel) and Material B (Pearlite steel) due to variation of load distance traveled

Distance Traveled [m]	Normal Load [kN]	Wear Volume [m^3]	
		Material A H = 270BHN	Material B H = 325BHN
200	20	3.08e-5	2.56e-5
400	30	9.24e-5	7.68e-5
600	40	1.85e-4	1.54e-4
800	50	3.08e-4	2.56e-4
1000	60	4.62e-4	3.84e-4
1200	70	6.47e-4	5.37e-4
1400	80	8.62e-4	7.17e-4
1600	90	1.11e-3	9.21e-4
1800	100	1.39e-3	1.15e-3
2000	110	1.69e-3	1.41e-3

Table 15.Wear rate and wear resistance value of Material A (Mn-steel) and Material B (Pearlite steel) due to distance variation

Distance Traveled [m]	Material A			Material B		
	Wear Volume [m3]	Wear Rate [m^3/m]	Wear resistance [m/m^3]	Wear Volume [m3]	Wear Rate [m^3/m]	Wear resistance [m/m^3]
200	3.08e-5	1.54e-7	6.49e6	2.56e-5	1.28e-7	7.81e6
400	9.24e-5	2.31e-7	4.33e6	7.68e-5	1.92e-7	5.21e6
600	1.85e-4	3.08e-7	3.25e6	1.54e-4	2.57e-7	3.89e6

800	3.08e-4	3.85e-7	2.60e6	2.56e-4	3.20e-7	3.12e6
1000	4.62e-4	4.62e-7	2.16e6	3.84e-4	3.84e-7	2.60e6
1200	6.47e-4	5.39e-7	1.86e6	5.37e-4	4.37e-7	2.29e6
1400	8.62e-4	6.16e-7	1.62e6	7.17e-4	5.12e-7	1.95e6
1600	1.11e-3	6.88e-7	1.45e6	9.21e-4	5.76e-7	1.74e6
1800	1.39e-3	7.72e-7	1.29e6	1.15e-3	6.39e-7	1.56e6
2000	1.69e-3	3.35e-6	3.98e5	1.41e-3	2.05e-6	4.88e5

b) Wear index I_w

Table 16.Wear Index of the two materials

Time [s]	Wear Index of Mn.steel	Wear Index of Pearlite steel
0	497.0766476	369.064225
2	84.00899712	106.7053779
4	1595.970413	0.11896337
6	1846.43461	425.3576034
8	1305.794405	496.0671284
10	1427.971703	1339.663343
12	18.64374125	1302.532136
14	32.12325977	1228.559647
16	168.2591265	440.8538085
18	1397.721768	540.6018599
20	1397.697868	216.3608021
22	1397.329851	608.349506
24	1397.340196	1138.940682
26	1568.846335	1485.773276
28	1402.122556	1599.96847
30	1398.507846	1398.576054

Table 17.Tabulation of K_w (I_w) expression for maximum wear index of the two materials

Material	$\mathbf{K_w (I_w)}$ [µg/m mm^2]
Manganese Steel	109571.302
Pearlite Steel	94315.048

c) Specific volume of material removed

Table 18.Specific volume of material removed

Material	Specific volume of material removed ($mm^3/m\ mm^2$)
Manganese Steel	0.014
Pearlite Steel	0.012

4.2. Discussion

4.2.1. Discussion on wear results

a) Discussion on wear of materials

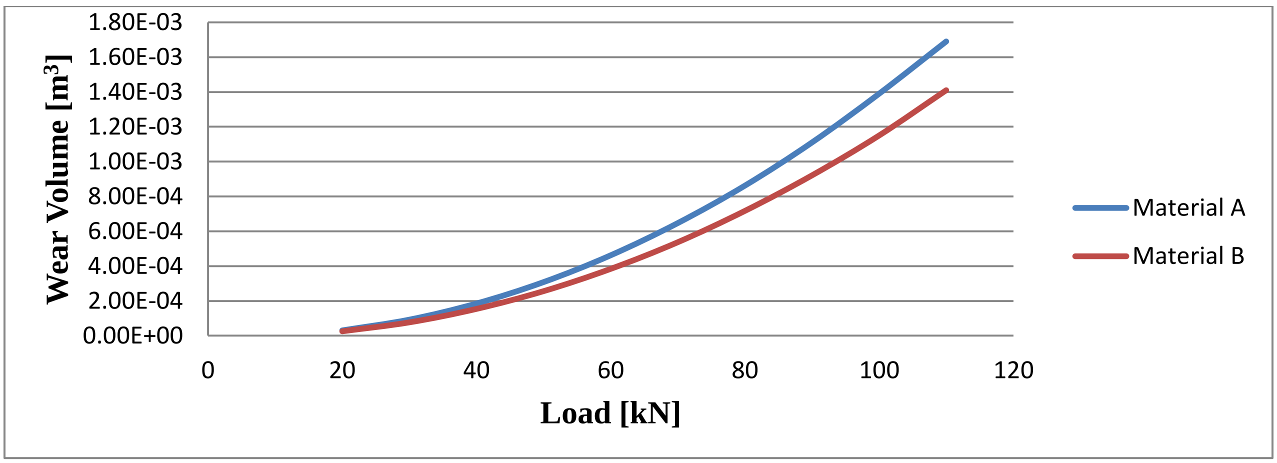

(a)

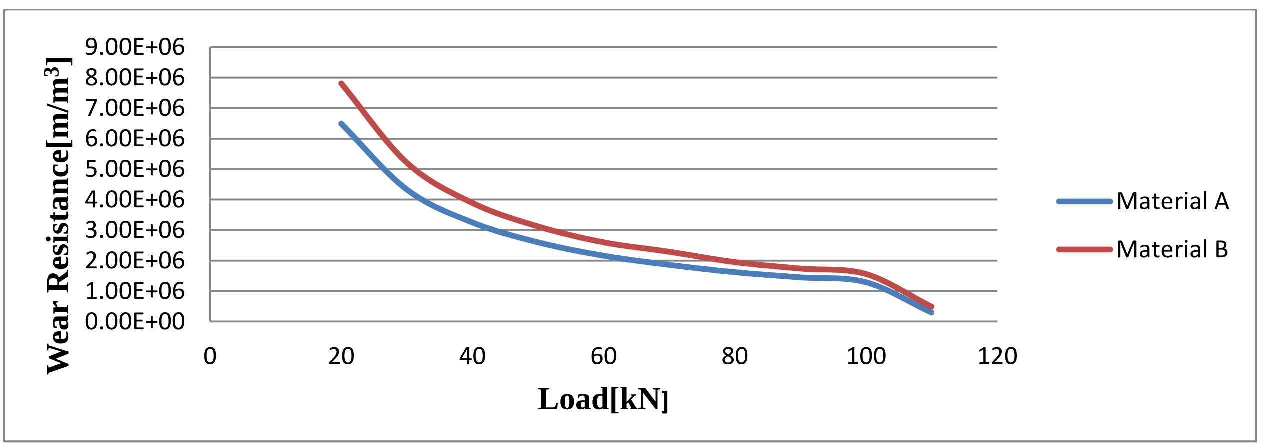

(b)

Figure 20.Effect of load (a) Wear Volume (b) Wear Resistance on Mn-steel (Material A) and Pearlite steel (Material B)

In the above graphs, the wear volume and the applied load for two different wheel materials are considered. The result shows that the wear volume on wheel-rail contact increases with increasing load as shown in figure 20 (a). Even though the wear volume increases for each wheel-rail contact materials, the wear volume on material A is greater than the wear volume on material B. On figure 20 (b) wear resistance vs load of materials are considered. In this graph wear resistance value on wheel-rail contact materials decrease with increasing load. On these graph wear resistance value of Pearlite steel (material B) is greater than Mn-steel (material A).

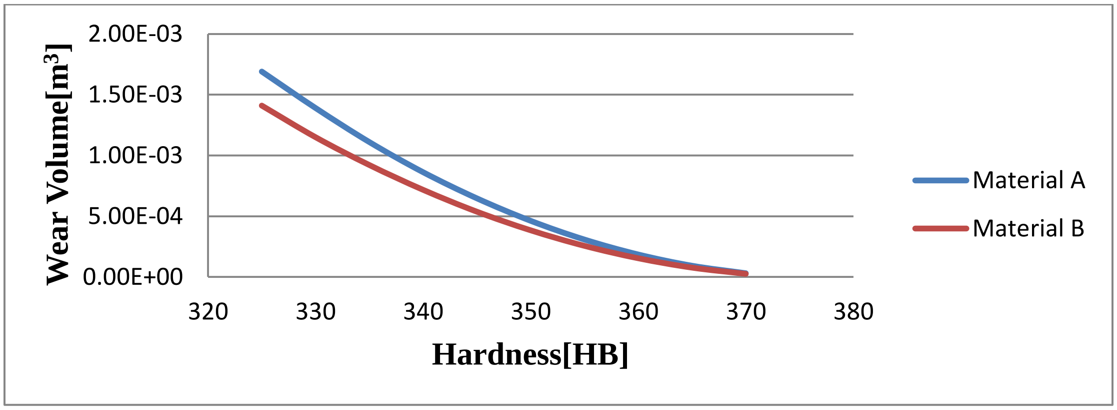

(a)

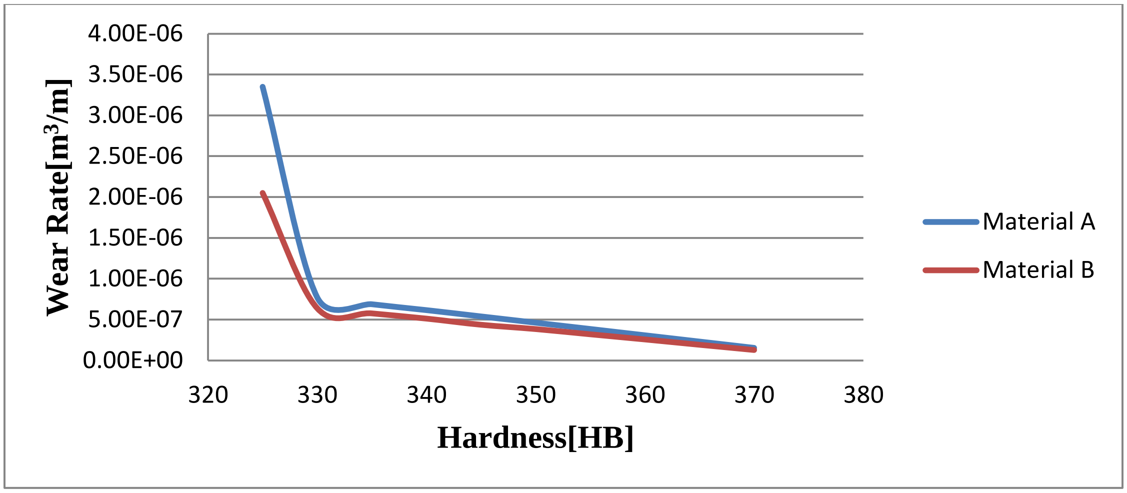

(b)

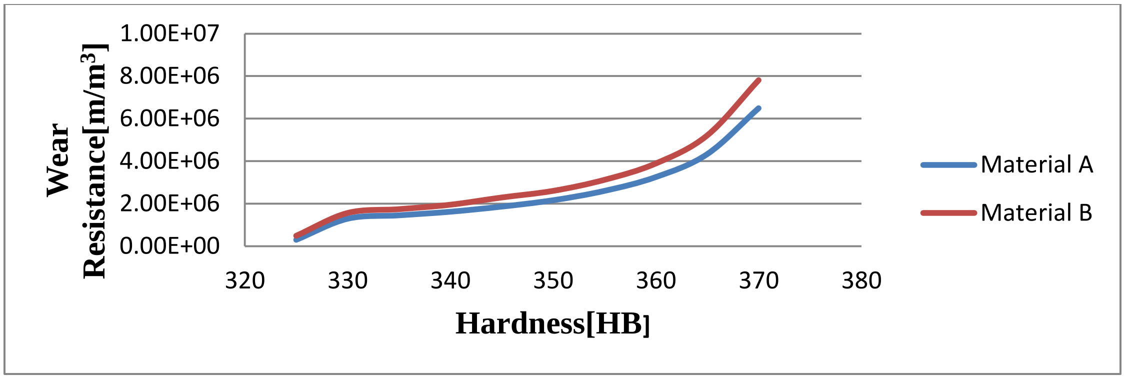

(c)

Figure 21.Effect of Hardness (a) Wear Volume (b) Wear Rate (c) Wear Resistance on Mn-steel (Material A) and Pearlite steel (Material B)

On figure 21 wear volume, wear rate and wear resistance values are considered with respect to hardness. On graph (a) wear volume decreases with increasing hardness. On the other hand wear rate of wheel-rail contact materials also decreases with increasing hardness as shown in graph (b). And wear resistance of wheel-rail contact materials increases with increasing hardness as shown on graph (c). In general, wear volume and wear rate of material A is greater than material B. And wear resistance of material A is better than material B with variation of hardness.

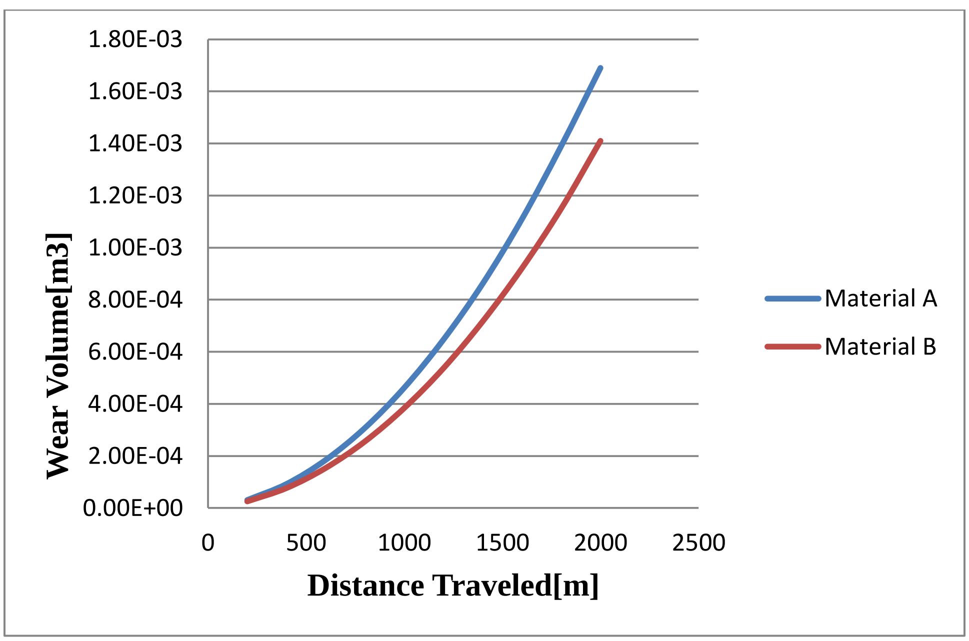

Figure 22.Wear volume vs Distance traveled on Mn-steel (Material A) and Pearlite steel (Material B)

In figure 22, the wear volume and the distance traveled are given for two different wheel materials. The result shows that the wear volume on wheel-rail contact increases with increasing distance traveled. Even though the wear volume increases for each wheel-rail contact, the wear volume on material A is greater than the wear volume on material B.

b) Discussion on wear index of materials

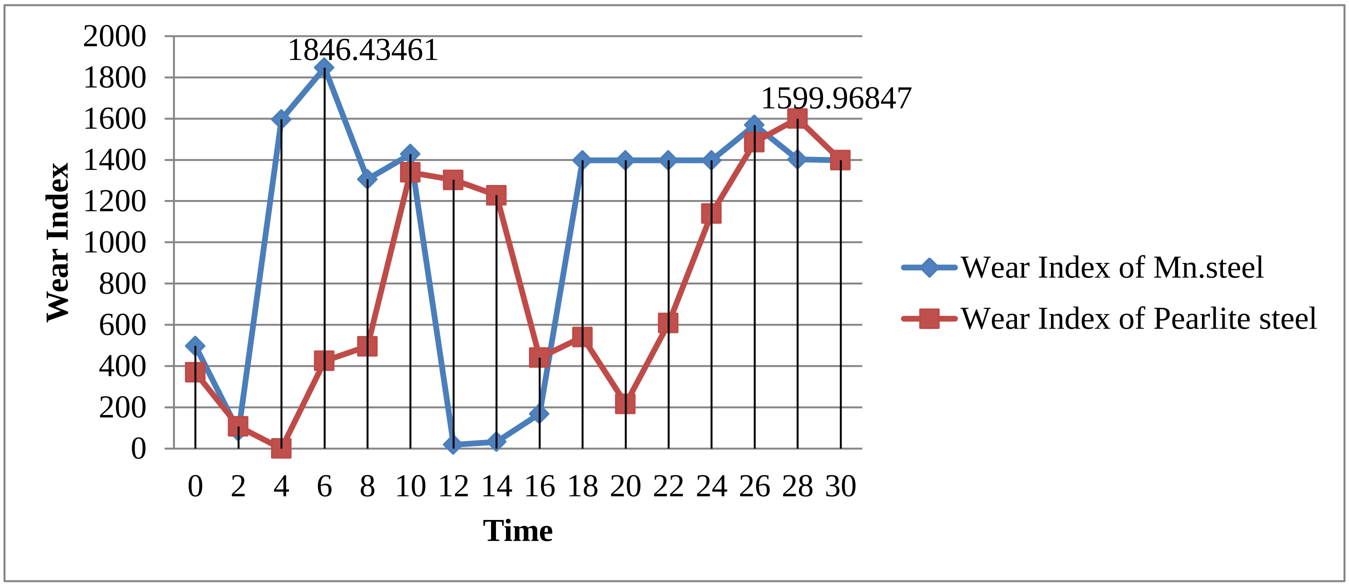

Figure 23.Wear index vs time graph

Figure 23 shows that the wear index calculated for the different creepages and creep forces. From the graph the highest wear index is found that 1846.43461 for manganese steel and 1599.96847 for Pearlite steel. This indicates that there is higher wear number in Manganese steel than Pearlite steel.

c) Discussion on specific volume of material removed

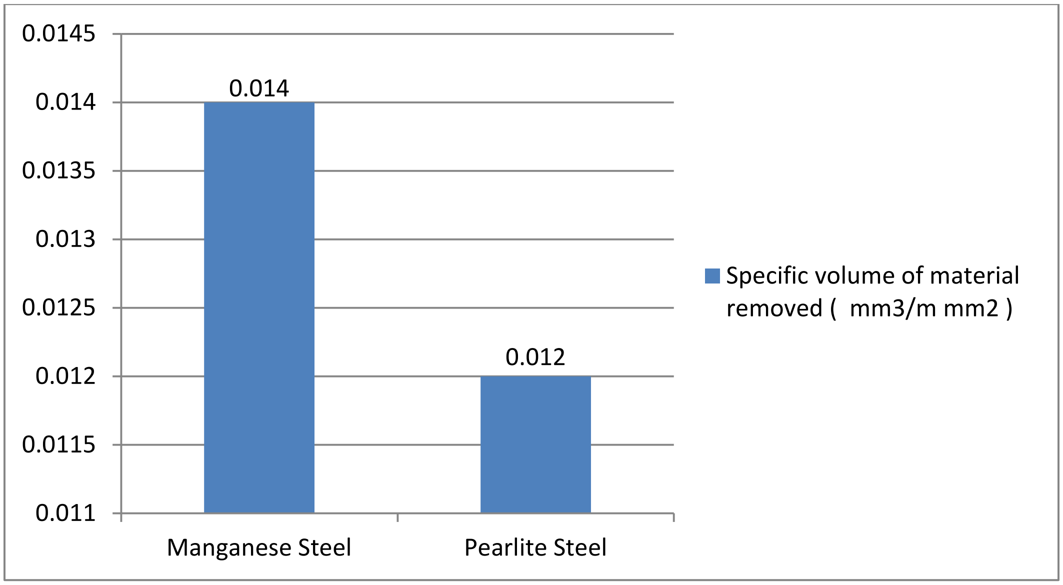

Figure 24.Specific volume of material removed

Figure 24 shows chart of Specific volume of material removed for Mn-steel and Pearlite steel. This indicates that Manganese steel has higher specific volume of material removed than Pearlite steel.

Generally, all the above information proves that Pearlite steel has better wear resistance than Manganese steel. This is because of the composition difference and physical properties of wheel-rail contact surface materials.

CHAPTER FIVE: CONCLUSION, RECOMMENDATION AND FUTURE WORK

5.1 Conclusion

The purpose of this thesis is to study wear resistance of wheel-rail contact surface materials. Since, the effect of several parameters, namely loads, motion, creeps, distance traveled and material hardness on railroad wheels is studied using the proposed model. The method of doing this thesis is numerical and analytical method. Based on such evaluation of wheel-rail wear materials, the following conclusions are drawn:-

- The wheel-rail contact surface of material B (Pearlite steel) has better wear resistance than material A (Manganese steel).
- Material B (Pearlite steel) provides improved performance and minimizes the wear and can provide longer life.
- Based on this study material B (Pearlite steel) is better than material A (Mn-steel) in wear resistance, wear volume and wear rate reduction and Pearlite steel is harder than Manganese steel.
- Generally, as the hardness of the wheel/rail, increase there is a better wear performance and in addition to hardness specific volume of material removed is highly depends on the density of the material.

5.2. Recommendation

Application of this thesis focuses on railway technology in the specific area of AALRT. Based on this thesis there are any other better steel material grades in terms of strength and wear resistance with better wheel and rail material combination. Due to this high strength and better wear resistance, materials like pearlite steel would bring a great benefit if used for railway project. Therefore, AALRT can use this pearlite steel.

5.3. Future Work

- Any interested researcher could do lots of tests using the test rig and software simulation in order to compare plenty of materials and identify the best one suitable for the condition in need.
- Any interested researcher can also do their thesis on improvement of wheel-rail contact surface materials using proper improvement methods.
- Any interested researcher could perform the economical aspect in terms of improving wheel-rail contact surface materials in relation to maintenance and replacement of wheel and rail components.
- We can't fully rely on software simulation results; due to this any interested researcher can do laboratory tests of wear resistance properties using wear test machines.

References

[1]. Ueda, M., Uchino, K., Matsushita, K., & Kobayashi, A., “Development of HE rails with high wear and damageresistance for heavy Haul Railways.” Nippon steel technical report. No.85 (2002).167-172.

[2]. Andersson, S., “Friction and wear simulation of the wheel–rail interface, royal Institute of Technology (KTH).” Stockholm: Sweden, (2009). 93-124.

[3]. Wa’ilRadwan All Tyfour, “Interaction between wear and rolling contact fatigue in pearlitic rail steels.” University of Leicester, April 1995.

[4]. Zmitrowicz, A., “Wear patterns and laws of wear.” Journal of theoretical and applied mechanics. 44, 2, Warsaw, (2006). pp. 219-253.

[5]. Braghin, F, Lewis, R, Dwyer-Joyce, R.S. and Bruni, S., “A mathematical model to predict railway wheel profile evolution due to wear.” Wear 261, UK, (2006). 1253–1264M

[6]. Innocenti, A., marini, L., Meli, E., Pallini, G. andRindi, A., “Prediction of wheel and rail profile wear oncomplex railway nets.” Florence University, Florence - Italy.

[7]. Stachowiak, G.W. and Batchelor, A.W., Engineering Tribology.

[8]. Wickens, A.H., “Fundamentals of rail Vehicle dynamics Guidance and Stability.” University of UK, 2003

[9]. Ozdemir, Y. and Voltr, P., “Analysis of the wheel and rail frictionless normal contact considering material parameters.” Pardubice, Czech Republic (2016) 15(2), 95-103

[10]. Lonsdale, C.,Prof. Bogacz, R., & Norton, M., “Application of Pressure Poured Cast Wheel Technology for European Freight Service, world congress on railway research.” State College, PA, USA, 2011.

[11]. Kasanna, R., Ajay, K., Naidu, M.K., S.Adinarayana, S. and Sudhakar, I., “Design and Analysis of Indian Wheel-RailAssembly for Super-Elevation.”International Journal for Research in Applied Science & Engineering Technology (IJRASET**)** Volume 5 Issue VII, July 2017.

[12]. Olofsson, U., and Lewis, R., “Tribology of the Wheel–Rail Contact, by Taylor & Francis Group, LLC.” Handbook of Railway Vehicle Dynamics. Stockholm: Sweden, (2006). 121-140.

[13]. Tseng, T.Y., “Dynamic Responses of Wheel-Rail Systems with Block Dampers.” Lincoln: Nebraska. (2016).

[14]. Galas, R., Omasta, M., Krupka, I., and Hartl, M. “Laboratory investigation of ability of oil-based friction modifiers to control adhesion at wheel-rail interface.” Faculty of Mechanical Engineering, Brno University of Technology. Brno: Czech Republic. (2016).

[15]. Matin Sh. Sichani. “Wheel-Rail Contact Modelling in Vehicle Dynamics Simulation.” Stockholm, Sweden. (2013).

[16]. Sathish Gandhi, V.C., Kumaravelan, R., Ramesh, S., Thanmanaselvi, M. &Sriram, K., “Performance Analysis of Wheel and Rail Contactby Nature of Material Characteristics– a Contact Mechanics Approach.” Vol. 18, No. 1 11–24, Lodz University of Technology. (2014).

[17]. Trzaska, Z., “Modeling of Energy Processes in Wheel-Rail ContactsOperating under Influence of PeriodicDiscontinuous Forces.” Journal of Transportation Technologies, 2, 129-143. (2012).

[18]. Buddhe, M., and Prof. Shaikh, S.M., “Analysis of rail-wheel contact stresses using finite element method in comparison with analytical solution.”International journal of innovations in engineering research and technology [IJIERT].ISSN: 2394-3696volume 3, Issue 8, Aug.-2016.

[19]. Spiryagin, M., Soo Lee, K., HeeYoo, H., Kashura, O., & Popov, S., “Numerical calculation of temperature in the wheel–rail flange contact and implications for lubricant choice, Wear 268, 287–293. Hanyang University,: South Korea (2010).

[20]. Jun, H.K., Lee,D.H., and Kim, D.S.“Calculation of minimum crack size for growth under rolling contact between wheel and rail.” Korea Railroad Research Institute: Republic of Korea. Wear 344-345 (2015) 46–57

[21]. Pombo, J., &Ambrósio, J., “A New Approach to Study the Wheel-Rail Contact Problem in Railway Dynamics.”Lisbon:Portugal. (2004).

[22]. Saini, G., Dr. Raj, T., & Sharma, A., “Design and analysis of rail track using solid works and ansys.” Volume No 03, Special Issue No. 01.Faridabad : India. (2015).

[23]. Okata, Y., “Design Technologies for Railway Wheels and Future Prospects.” Nippon steel &sumito metal technical report No. 105, December (2013).

[24]. K.D. Vo, A.K. Tieu, H.T. Zhu, P.B. Kosasih, “A 3D dynamic model to investigate wheel-rail contact under High and low adhesion.” International Journal of Mechanical Sciences, http://dx.doi.org/10.1016/j.ijmecsci.2014.05.007

[25]. P.K. Sarkar, P.K., and Ranjan, V., "An Approximate Analysis for Hertzian Elliptical Wheel-Rail Contact Problem." Proceedings of the 1st International and 16th National Conference on Machines and Mechanisms (iNaCoMM2013), IIT Roorkee, India, Dec 18-20 (2013).

[26]. Al-Samarai1, R.A., Haftirman, Ahmad, K. R., and Al-Douri, Y.,"Effect of Load and Sliding Speed on Wear and Friction ofAluminum– Silicon Casting Alloy." International Journal of Scientific and Research Publications, Volume 2, Issue 3, Perlis : Malaysia March (2012). ISSN 2250-3153.

[27]. L. Ma, et al., "Study on wear and rolling contact fatigue behaviors of wheel/rail materials under different slip ratio conditions." Wear (2016). http://dx.doi.org/10.1016/j.wear.2016.04.028

[28]. Axén, N., Hogmark, S., and Jacobson, S., "Friction and Wear Measurement Techniques." Modern tribology handbook.Uppsala University, by CRC Press LLC, (2001).

[29]. FaridMovassagh-Alanagh, Amir Abdollah-zadeh, MahmoodAliofkhazraei and Mohammad Abedi, "Improving the Wear and Corrosion Resistance of Ti–6Al–4V Alloy by Deposition of TiSiNNanocomposite Coating with Pulsed-DC PACVD." Wear, http://dx.doi.org/10.1016/j.wear.2017.07.009

[30].RoviraCardete, A.; RodaBuch, A.; Marshall, M.; Brunskill, H.; Lewis, R. "Experimental and numerical modelling of wheel rail contact and wear." Wear. 271(5-6):911- 924. (2011). doi:10.1016/j.wear.2011.03.024.

[31]. Clayton, P., "Tribological aspects of wheel-rail contact: a review of recent experimental research." Oregon Graduate Institute of Science and Technology, Department of Materials Science and Engineering, Portland, OR 97291-1000, USA, Wear 191 (1996) 17&183

[32]. Ajay Kapoor, et al., "Tribology of Rail Transport." The University of Sheffield, by CRC Press LLC, (2001).

[33]. Madler, K. and Bannasch, M., "Materials used for wheels in rolling stock." Germany.

[34]. Markov, D., "Laboratory tests for wear of rail and wheel steels." Deparhnent of Metals, Railway Research Institute, Mitishitdaj 3-10, Moscow, Russia, Wear 181-183 (1995) 678-686.

[35]. Tatsumi, K, Mineyasu, T., and Minoru, H., "Development of SP3 Rail with High Wear Resistance and Rolling Contact Fatigue Resistance for Heavy Haul Railways." JFE Technical report.No. 16 (Mar. 2011).

[36]. Yokoyama, H., Mitao, S.,, and Yamamoto, S. “Wear and Rolling Contact Fatigue Behavior in Pearlitic and Bainitic Rail Steels.” Materials & Processing Research Center, NKK Corporation, Fukuyama 721-8510, Japan, 7th International Heavy Haul Conference, (2001).

[37]. Albert0 J. Perez-Unzueta and John H. Beynon, “Microstructure and wear resistance of pearlitic rail steels.” Leicester : UK, Wear, 162-164 (1993) 173 - 182.

[38]. Osamu Kondo, O. and Yamazaki, Y. “Simulation Technology for Railway Vehicle Dynamics.” Nippon steel &sumito metal technical report No. 105, December (2013).

[39]. Shevtsov, I.Y., “Wheel/Rail Interface Optimisation.” Section of Road and Railway Engineering. Delft University of Technology, The Netherlands. ISBN 978-90-8570-303-7.(2008).

[40]. Auciello, J., Ignesti, M., Marini, L., Meli, E. and Rindi, A. “Development of a model for the analysis of wheel wearin railway vehicles.”Meccanica (2013) 48:681–697.

[41]. Joao, “Application of computational tools to study the influence of worn wheel on railway vehicle dynamics.” 2012, pp.51-61

[42]. Ethiopian Railway Corporation, technical specification of vehicle

Appendices

Appendix A: Chemical composition test results

Table A1: Chemical composition test results of wheel material

SPECTRO AMETEK MATERIALS ANALYSIS DIVISION

AKAKI BASIC METALS INDUSTRY SPECTRO TEST RESULTS

Sample Result Name	Type	Measure Date Time	Recalculation Date Time	Origin	Method Name	Method Version	Operator Name	Correction Type	Type Corr Sample Name
	Mn-steel	1/3/2018 11:45:12 AM	1/3/2018 11:45:45 AM	Measured	Fe-50-MO			None	

Check Type	Check Status	Grade Verification Name	Grade Verification Similarity	Grade Search Name	Grade Search Similarity
None	Not Used		0%		0%
Sample Name					

Elements Conc.

Meas.	C	Si	Mn	P	S	Cr	Mo	Ni	Al	Co
	%	%	%	%	%	%	%	%	%	%
	Conc.	Conc.	Conc.	Conc.	Conc.	Conc.	Conc.	Conc.	Conc.	Conc.
<x>	0.50	0.28	0.80	<0.05	<0.05	0.02	0.001	<0.005	0.012	0.006

Meas.	Cu	Nb	Ti	V	Sn	Fe				
	%	%	%	%	%	%				
	Conc.	Conc.	Conc.	Conc.	Conc.	Conc.				
<x>	0.031	<0.005	0.004	<0.002	0.004	98.249				

Tested by Asegedu
25/4/10

Abere Dessie
(Cap.)
Quality Management Head

Table A2: Chemical composition test results of rail material

	HIBRET MANUFACTURING AND MACHINE BUILDING INDUSTRY	DOC. No.HMMBI HMMBI/ / SPI/LB/-02	
	Chemical composition Laboratory Test Result Form	Issue No. 01	Page 1 of 1

Date: 26/06/10

Requested by: Teshome Meku

Sample type: STEEL

Purpose: IDENTIFICATION

S/N	Sample Name	Chemical composition										
		C	Si	Mn	P	S	Cr	Mo	Ni	Cu	V	Fe
1	Flat	0.60	0.35	1.20	<0.05	<0.05	0.20	0.001	<0.005	0.035	0.042	97.570

Prepared by: Diribe
Sign:
Date: 26/06/10

Checked by: Alemitu
Sign:
Date: 26/06/10

Approved by: DEGADA
Sign:
Date: 26/06/10

Hibret Manufacturing & Machine Building Industry

Appendix B: Wheel Data Measurements of AALRT Vehicles

					pre-measurement					post-measurement						
No.	Date	mileage	vehicle No.	wheelset No.	diameter difference	diameter		flange thickness		diameter difference	diameter		flange thickness		total re-profiled wheelset	remark
						left	right	left	right		left	right	left	right		
1	3-9/2/2016	4888	104	1	0.08	660.66	660.58	23.25	23.26	-	-	-	-	-		burn on wheel thread
				2	0.1	660.54	660.64	23.18	23.3	-	-	-	-	-		
				3	0.67	659.87	660.55	22.4	22.97	1.77	650.17	651.94	19.75	19.96	1	
				4	0.21	660.45	660.66	22.95	22.51	0.06	652.53	652.59	20.6	21.03	2	
				5	0.15	660.48	660.63	23.07	23.19	-	-	-	-	-		
				6	0.06	660.47	660.53	23.53	23.36	-	-	-	-	-		
2	15-18/03/2016	6065	104	1	0.14	660.63	660.49	23.27	23.13	-	-	-	-	-		burn on wheel thread
				2	0.04	660.51	660.55	22.95	23.25	-	-	-	-	-		
				3	0.76	651.06	651.82	19.62	19.74	1.36	649.92	651.28	19.58	19.75	3	
				4	0.01	652.48	652.46	20.27	20.79	0.16	651.36	651.2	20.21	20.05	4	
				5	0.13	660.46	660.6	23.19	23.34	-	-	-	-	-		
				6	0.22	660.51	660.29	23.4	23.15	-	-	-	-	-		
3	25/03/2016 to 11/04/2016	30478	119	1	0.1	660	659.9	20.24	21	-	-	-	-	-		scratch on wheel thread
				2	0.15	659.94	660.1	20.82	20.81	-	-	-	-	-		
				3	0.01	660.36	660.37	19.77	20.4	0.3	655.15	655.45	22.28	22.3	5	
				4	0.49	660.79	660.29	20.18	19.45	0.39	656.82	656.43	19.65	19.71	6	
				5	0.08	660.13	660.05	20.75	20.62	-	-	-	-	-		
				6	0.09	660.13	660.03	21.08	20.83	-	-	-	-	-		
4	7-8/5/2016	no	213	1	0.53	659.07	659.6	16.74	17.04	0.01	639.73	639.73	19.88	19.86	7	wheel flange thickness
				2	0.84	659.34	658.5	17.5	14.61	0.16	635.17	635.01	19.41	19.57	8	
				3	-	-	-	-	-	-	-	-	-	-		
				4	-	-	-	-	-	-	-	-	-	-		
				5	0.1	659.69	659.79	15.7	17.56	-	-	-	-	-		
				6	0.35	659.54	659.19	17.77	15.49	-	-	-	-	-		
5	8-10/6/2016	26848	211	1	0.14	659.87	660.01	19.11	19.42	-	-	-	-	-		wheel flange thickness
				2	0.32	659.97	659.65	17.89	18.32	-	-	-	-	-		
				3	0.61	651.4	652.01	19.09	18.98	0.01	640	639.99	18.87	18.31	9	
				4	0.71	660.83	660.12	19.09	13.24	0.35	634.84	635.18	19.52	18.74	10	
				5	0.21	659.93	660.14	19.19	19.35	-	-	-	-	-		
				6	0.11	659.91	660.03	19.46	17.03	-	-	-	-	-		
6	11-12/6/2016	56447	209	1	0.2	659.18	659.38	15.34	17.24	0.41	650.82	651.23	17.3	17.3	11	scratch on wheel thread
				2	0.09	659.42	659.33	15.97	15.58	0.04	650.91	650.95	17.62	17.69	12	
				3	0.16	660.16	660	17.21	17.5	0.11	648.69	648.58	20.02	20.03		
				4	0.08	659.8	659.88	15.28	16.31	0.14	648.47	648.61	19.08	18.99		
				5	0.23	659.36	659.59	17.34	17.27	-	-	-	-	-		
				6	0.02	659.28	659.3	16.43	15.18	0.22	654.08	654.3	17.01	16.85	13	
7	12-14/06/2016	35955	216	1	0.18	659.61	659.79	16.81	17.78	0.4	649.82	650.23	19.17	19.16	14	wheel flange thickness
				2	0.07	659.74	659.8	15.25	14.45	0.12	646.73	646.61	17.94	17.87		
				3	0	660.32	660.32	18.13	17.95	-	-	-	-	-		
				4	0.07	660.35	660.29	18.5	18.46	-	-	-	-	-		
				5	0.23	659.78	660.01	17.49	16.6	0.17	648.19	648.37	20.21	19.9	15	
				6	0.02	659.76	659.74	18.28	14.84	0.6	648.18	648.78	18.58	18.35	16	
8	14-16/6/2016	44026	212	1	0.04	659.66	659.63	16.06	17.5	0.03	641.17	641.14	19.86	19.7	17	
				2	0.33	659.73	659.4	17.02	13.66	0.07	638.31	638.38	18.41	18.4	18	
				3	0.01	660.12	660.13	16.49	17.69	0.38	653.41	653.03	18.42	18.6	19	
				4	0.12	660.09	660.21	17.48	17.62	0.26	653.65	653.39	19.51	19.53	20	
				5	0.54	659.34	659.88	16.63	19.38	0.05	653.52	653.58	18.36	18.36	21	
				6	0.06	659.55	659.49	16.41	16.93	0	653.14	653.15	18.14	18.07	22	
9	17-18/6/2016	6518	107	1	0.25	659.56	659.32	19.92	20.31	-	-	-	-	-		wheel flange thickness
				2	0.04	659.46	659.51	19.75	19.65	-	-	-	-	-		
				3	0.3	660.1	660.39	18.2	16.09	0.31	649.78	650.09	18.68	18.87	23	
				4	0.32	660.09	660.41	17.95	14.81	0.32	650.08	650.13	18.03	17.86	24	
				5	0.36	659.73	659.37	19.28	19.51	-	-	-	-	-		
				6	0.07	659.51	659.44	20.08	20.31	-	-	-	-	-		
10	18-21/06/2016	35568	217	1	0.13	656.07	656.19	16.65	17.01	0.16	652.04	652.2	17.13	17.61	25	
				2	0.06	659.73	659.67	17.61	16.83	0.31	655.46	655.77	18.27	18.22	26	
				3	0.19	651.07	650.87	18.04	18.45	0.06	641.08	641.14	19.55	19.86	27	
				4	0.11	645.06	644.95	16.66	16.82	0.05	640.98	641.03	17.02	17.15	28	
				5	0.21	659.73	659.94	18.32	18.89	-	-	-	-	-		
				6	0.05	659.65	659.7	17.52	16.36	-	-	-	-	-		
11	4-24/06/2016	53109	206	1	0.39	659.05	659.44	16.25	17.22	0.16	649.24	649.4	18.97	19.38	29	wheel flange thickness
				2	0.06	659.3	659.24	16.87	15.14	0.16	648.08	648.21	18.04	18.57	30	
				3	0.29	660.31	660.02	14.01	15.07	0.16	639.04	639.31	18.56	18.8	31	
				4	0.23	660.21	659.98	12.45	14.48	0.16	637.63	637.96	17.68	17.94	32	
				5	0.21	659.35	659.55	17.35	16.63	0.16	653.16	653.6	17.9	18.01	33	
				6	0.02	659.44	659.46	15.92	15.36	0.16	653.2	653.42	17.61	17.91	34	
12	24-26/06/2016	45540	115	1	0.17	659.66	659.49	20.62	19.75	-	-	-	-	-		wheel flange thickness
				2	0.18	659.83	659.65	20.39	20.28	-	-	-	-	-		
				3	0.41	659.89	660.3	19.2	15.13	0.92	635.37	636.3	20	20.79	35	
				4	0.32	659.94	660.26	19.77	14.08	0.37	635.29	635.66	19.25	19.38	36	
				5	0.22	659.87	659.65	20.71	20.59	-	-	-	-	-		
				6	0.18	659.6	659.41	20.45	19.91	-	-	-	-	-		
13	27/6-1/7/2016	49030	205	1	0.11	659.42	659.53	16.71	16.54	0.44	639.66	640.09	20.31	20.09	37	wheel flange thickness
				2	0.02	659.62	659.64	17.48	13.48	0.47	637.17	637.64	17.56	17.56	38	
				3	0.04	660.15	660.19	17.38	18.24	-	-	-	-	-		
				4	0.08	659.96	660.04	16.38	17.37	-	-	-	-	-		
				5	0.04	659.55	659.59	16.48	16.59	-	-	-	-	-		
				6	0.08	659.61	659.69	17.59	18.51	-	-	-	-	-		

14	3-7/7/2016	54471	218	1	0.3	659.29	659.59	13.7	16.65	0.24	642.86	643.11	17.65	17.59	39	wheel flange thickness
				2	0.15	659.29	659.44	14.16	13.86	0.32	643.27	642.96	17.58	17.67	40	
				3	0.01	660.19	660.21	17.08	16.14	0.24	636.55	636.79	19.55	19.72	41	
				4	0.16	660.08	659.92	14.11	12.83	0.32	637.96	638.28	17.69	17.78	42	
				5	0.53	659.12	659.65	18.38	18.06	0.03	647.98	647.95	21.11	20.85	43	
				6	0.41	658.94	659.34	16.02	15.26	0.22	648.16	647.94	17.83	17.78	44	
15	08-11/07/2016	47312	215	1	0.44	659.56	660	17.07	17.93	0.31	640.76	641.07	20.97	21.08	45	wheel flange thickness
				2	0.06	659.79	659.73	15.46	13.46	0.1	642.02	642.12	17.44	17.55	46	
				3	0.09	660.33	660.41	18.05	16.75	0.3	645.14	645.44	19.71	19.94	47	
				4	0.18	660.1	660.28	17.09	15.45	0.21	644.17	644.38	18.82	18.81	48	
				5	0.02	659.79	659.81	16.54	16.65	-	-	-	-	-		
				6	0.17	659.79	659.62	16.17	16.03	-	-	-	-	-		
16	13-14/07/2016	22282	207	1	0.19	659.96	660.15	18.63	20.02	0.1	655.17	655.27	19.59	19.84	49	
				2	0.08	660	659.92	18.48	17.54	0.1	654.87	654.76	18.91	18.96	50	
				3	0.01	660.32	660.33	19.54	19.36	-	-	-	-	-		
				4	0.06	660.26	660.32	18.13	18.11	-	-	-	-	-		
				5	0.12	659.98	660.1	19.37	18.82	-	-	-	-	-		
				6	0.06	659.94	660	19.06	17.62	-	-	-	-	-		
17	15-27/07/2016	43452	208	1	0.07	659.43	659.5	16.34	17.53	0.29	637.93	638.21	20.11	20.24	51	wheel flange thickness
				2	0.22	659.56	659.78	13.45	18.34	0.19	635.4	635.21	17.41	17.75	52	
				3	0.15	660.14	660.29	17.05	15.44	0.1	640.15	640.05	18.58	18.78	53	
				4	0.06	660.19	660.12	17.28	14.47	0.23	639.02	638.79	18.3	18.3	54	
				5	0.12	659.67	659.56	18.68	16.96	0.19	645.95	645.76	19.68	19.82	55	
				6	0.2	659.36	659.55	17.09	15.99	0.07	645.78	645.86	18.86	18.9	56	
18	17-18/08/2016	45551	114	1	0.12	659.86	659.74	19.6	20.48	-	-	-	-	-		
				2	0.1	659.85	659.95	20.29	20.47	-	-	-	-	-		
				3	0.25	660.3	660.05	18.52	19.71	0.35	655.78	655.43	18.67	19.38	57	
				4	0.25	660.27	660.02	18.4	19.63	0.58	655.16	655.75	19.35	19.26	58	
				5	0.09	659.88	659.79	19.68	20.34	-	-	-	-	-		
				6	0.12	659.79	659.67	21.11	19.99	-	-	-	-	-		
19	9-22/08/2016	51662	210	1	0.32	659.02	659.34	16.12	16.36	0.29	642.73	642.44	18.99	18.99	59	wheel flange thickness
				2	0.24	659.44	659.2	16.3	14.39	0.61	642.23	641.63	17.75	18.09	60	
				3	0.23	660.06	660.3	15.52	14.21	0.39	640.74	641.13	17.39	17.46	61	
				4	0.21	650.68	650.89	17.51	17.45	0.05	642.57	642.52	18.1	18.44	62	
				5	0.2	659.25	659.45	16.4	16.93	0.15	646.23	646.37	18.02	18.11	63	
				6	0	659.15	659.16	16.38	14.98	0.41	645.96	645.55	17.27	17.58	64	
20	23-25/08/2016	40415	108	1	0.42	659.94	659.52	20.44	20.4	-	-	-	-	-		
				2	0.03	659.67	659.64	19.94	19.66	-	-	-	-	-		
				3	0.21	660.49	660.28	18.59	17.81	0.65	654.65	655.3	18.52	18.82	65	
				4	0.13	660.15	660.28	17.9	16.94	0.23	654.01	654.54	18.54	18.87	66	
				5	0.38	659.94	659.56	19.64	19.67	-	-	-	-	-		
				6	0.37	659.9	659.53	20.05	20.08	-	-	-	-	-		

21	25-30/08/2016	45551	111	1	0.44	659.16	658.73	18.52	18.79	-	-	-	-	-		wheel flange thickness
				2	0.19	658.93	658.74	18.05	18.59	-	-	-	-	-		
				3	0.53	659.83	660.36	17.14	13.11	0.31	636.12	636.43	17.94	17.76	67	
				4	0.56	659.73	660.29	17.26	13.04	0.51	635.31	635.82	17.23	16.99	68	
				5	0.09	659.88	659.79	19.68	20.34	-	-	-	-	-		
				6	0.12	659.79	659.67	21.11	19.99	-	-	-	-	-		
22	05-07/09/2016	54807	110	1	0.22	659.34	659.12	18.71	19.11	-	-	-	-	-		wheel flange thickness
				2	0.23	659.41	659.18	18.86	18.64	-	-	-	-	-		
				3	0.31	659.99	660.31	17.13	14.58	1.1	637.47	636.36	18.33	18.75	69	
				4	0.58	659.8	660.37	17.02	13.09	0.22	636.5	636.28	18.24	18.07	70	
				5	0.5	659.79	659.29	19.71	18.67	-	-	-	-	-		
				6	0.25	659.19	658.95	18.97	18.06	-	-	-	-	-		
23	09-16/09/2016	61474	219	1	0.42	658.83	659.26	13.78	15.73	0.22	632.77	633	18.46	18.34	71	wheel thread scratch & wheel flange thickness
				2	0.11	659.02	658.91	14.12	12.97	0.27	631.54	631.8	17.84	17.87	72	
				3	0.26	659.88	660.15	14.94	14.18	0.96	630.83	630.91	18.84	18.42	73	
				4	0.12	659.95	659.83	14.97	13.22	0.75	631.27	631.42	18.3	17.86	74	
				5	0.52	659.04	659.56	15.01	13.23	0.13	634.26	634.4	17.92	17.96	75	
				6	0.43	658.92	659.36	13.68	12.55	0.19	633.38	633.19	17.94	18.11	76	
24	14-15/11/2016	76430	109	1	0.11	658.81	658.7	18.71	18.59	-	-	-	-	-		wheel flange thickness
				2	0.05	658.86	658.81	19.16	18.28	-	-	-	-	-		
				3	0.49	660.35	659.86	12.45	17.42	0.65	629.45	628.8	17.88	18	77	
				4	0.31	660.17	659.86	13.68	16.42	0.27	629.68	629.41	19.6	19.49	78	
				5	0.19	659.16	658.97	18.65	18.27	-	-	-	-	-		
				6	0.09	658.89	658.8	19.18	18.24	-	-	-	-	-		
25	16-18/11/2016	78624	218	1	0.26	641.85	642.11	13.65	13.97	0.12	618.12	618	18.08	18.17	79	wheel flange thickness
				2	0.12	642.28	642.16	14.71	14.09	0.06	616.53	616.59	20.35	19.53	80	
				3	0.16	612.41	612.25	19.62	19.74	0.16	612.41	612.25	19.62	19.74	81	
				4	0.32	637.64	637.96	13.25	13.07	0.18	609.91	609.73	17.89	18.05	82	
				5	0.04	626.7	626.74	20.9	20.87	0.04	626.7	626.74	20.9	20.87	83	
				6	0.13	647.16	647.03	14.81	14.29	0.11	626.16	626.05	17.99	17.93	84	
26	19to21/11/2016	66522	216	1	0.15	648.92	649.07	16.52	16.1	0.3	623.18	623.48	20	20.09	85	wheel flange thickness
				2	0.07	645.61	645.54	15.96	15.02	0	622.13	622.13	18.46	18.4	86	
				3	0.07	660.03	659.96	17.86	16.84	-	-	-	-	-		
				4	0.15	659.99	659.84	18.15	17.53	-	-	-	-	-		
				5	0.08	647.3	647.22	18.47	16.75	0.05	627.07	627.02	19.69	19.12	87	
				6	0.06	647.24	647.3	16.6	14.75	0.01	625	624.99	18.38	18.36	88	
27	24/11/2016	26848	211	1	-	-	-	-	-	-	-	-	-	-	-	scratch on thread and abnormal wheel flange profile
				2	-	-	-	-	-	-	-	-	-	-	-	
				3	0.06	639.74	639.8	18.86	17.79	0.09	630.25	630.25	19.12	19.3	89	
				4	0.42	634.87	635.29	19.28	18.19	0.2	629.22	629.42	18.16	18.15	90	
				5	-	-	-	-	-	-	-	-	-	-	-	
				6	-	-	-	-	-	-	-	-	-	-	-	

28			217	1	0.06	651.32	651.26	15.26	15.04	0.11	625.02	625.13	19.14	19.36	91	wheel flange thickness
				2	0.01	654.81	654.82	17.26	16.56	0.07	625.34	625.41	20.76	20.74	92	
				3	0.37	640.7	641.07	17.08	16.19	0.02	616.36	616.34	19.46	19.61	93	
				4	0.2	640.46	640.66	14.77	13.67	0.33	614.21	614.54	18.18	18.31	94	
				5	0.36	659.25	659.61	18.39	18.23	0.22	642.37	642.59	20.91	20.84	95	
				6	0.03	659.23	659.26	17.59	15.38	0.14	641.21	641.36	18.53	18.44	96	
29	30/11/2016	69044	115	1	0.37	659.14	658.77	21.41	19.37	-	-	-	-	-		wheel flange thickness
				2	0.06	659.12	659.06	21.15	19.99	-	-	-	-	-		
				3	4.69	635.12	635.91	19.34	15.24	0.32	607.06	607.58	19.63	19.55	97	
				4	0.45	634.9	635.35	18.52	14.09	0.02	605.31	605.33	18.78	18.71	98	
				5	0.23	659.25	659.02	21.45	20.51	-	-	-	-	-		
				6	0.16	658.82	658.66	20.98	19.82	-	-	-	-	-		
30	12/5/2016	57012	220	1	0	659.3	659.3	18.42	17.65	-	-	-	-	-		wheel flange thickness
				2	0.03	659.72	659.3	17.82	16.97	-	-	-	-	-		
				3	0.22	659.89	660.11	17.64	15.57	0	636.33	636.33	19.69	19.83	99	
				4	0.1	659.82	659.92	18.55	18.69	0	636.29	636.29	18.55	18.69	100	
				5	0.33	658.98	659.31	18.23	17.66	-	-	-	-	-		
				6	0.02	659.12	659.1	18.34	16.64	-	-	-	-	-		
31	13-14/12/2016		219	1	0.22	632.52	632.74	20.21	19.32	-	-	-	-	-		scratch on wheel thread
				2	0.23	631.31	631.54	19.67	19.2	-	-	-	-	-		
				3	0.11	630.62	630.73	20.43	19.41	0.07	626.67	626.6	19.34	19.36	101	
				4	0.16	631.11	631.27	19.88	19.85	0.04	628.28	628.32	19.42	19.48	102	
				5	0.02	634.04	634.02	19.75	18.92	-	-	-	-	-		
				6	0.45	633.21	632.76	19.45	19.17	-	-	-	-	-		
32	15-20/12/2016	52732	108	1	0.43	659.65	659.23	21.29	20.63	0.01	653.12	653.13	21.54	21.61	103	scratch on wheel thread
				2	0.04	659.25	659.29	20.87	19.87	0.12	653.12	653.24	20.67	20.74	104	
				3	0.73	654.36	655.09	18.78	18.65	-	-	-	-	-		
				4	0.43	653.65	654.04	18.6	18.04	-	-	-	-	-		
				5	0.32	659.5	659.18	20.71	19.97	-	-	-	-	-		
				6	0.31	659.48	659.17	20.98	20.43	-	-	-	-	-		
33	22-28/12/2016	75028	206	1	0.07	648.45	648.52	17.08	16.77	0.02	625.49	625.48	20.46	20.34	105	wheel flange thickness
				2	0.06	647.39	647.45	16.57	15.74	0.05	623.99	623.93	19.81	19.69	106	
				3	0.15	638.77	638.92	15.41	15.38	0.23	615.7	615.47	19.21	19.21	107	
				4	0.23	637.33	637.56	14.6	14.34	0.02	615.31	615.29	18.44	18.28	108	
				5	0.14	652.58	652.72	16.52	16.09	0.0.15	625.91	626.06	20.72	20.44	109	
				6	0.23	652.36	652.59	16.07	15.47	0.33	625.06	624.73	19.94	19.91	110	
	>>> flange increase indicates the value added on list flange thickness															
	>>> diameter reduction indicates the total amount lathed from pre-measured diameter size															
	>>> factor of diameter reduction the amount of diameter reduction for unit increase or flange thickness															
	>>> pre-measurement refers the measurement before lathing															
	>>> post-measurement refers the measurement after lathing															
	>>> "-" refers wheels those not lathed															

Appendix C: SIMPACK results

Table C1: Longitudinal and Lateral Creepage

Curve Properties

General | Source | Info

Number of values: 16

X-Start:	0	Y-Start:	0.329185
X-End:	30	Y-End:	0.00787917
X-Min:	0	Y-Min:	0
X-Max:	30	Y-Max:	0.329185

	Time	Longitudinal Creepage of Mn-steel
1	0	0.329185
2	2	0.294144
3	4	0
4	6	0.199003
5	8	1.90496e-06
6	10	0.0955539
7	12	0.0116855
8	14	0.00524612
9	16	1.13738e-07
10	18	0.00299102
11	20	0.0030256
12	22	2.80227e-07
13	24	1.10716e-06
14	26	0.0439277
15	28	0.037475
16	30	0.00787917

Curve Properties

General | Source | Info

Number of values: 16

X-Start:	0	Y-Start:	0.329189
X-End:	30	Y-End:	0.00836782
X-Min:	0	Y-Min:	0
X-Max:	30	Y-Max:	0.329189

	Time	Longitudinal Creepage of Pearlite steel
1	0	0.329189
2	2	0.313952
3	4	0
4	6	0.224961
5	8	0.218385
6	10	0.153694
7	12	0.147224
8	14	0.000779776
9	16	0.000719857
10	18	0.011521
11	20	0.00508919
12	22	2.86791e-05
13	24	3.43015e-05
14	26	0.00595952
15	28	0.00601162
16	30	0.00836782

Curve Properties

General | Source | Info

Number of values:	16		
X-Start:	0	Y-Start:	0.0144482
X-End:	30	Y-End:	0.0936588
X-Min:	0	Y-Min:	0
X-Max:	30	Y-Max:	0.0936588

	Time	Lateral Creepage of Mn-steel
1	0	0.0144482
2	2	0
3	4	0.000412778
4	6	4.6054e-05
5	8	1.02137e-05
6	10	9.98144e-06
7	12	0.0060323
8	14	0.00581535
9	16	0.000125343
10	18	0.00983399
11	20	0.0100129
12	22	0.0498172
13	24	0.0500604
14	26	0.0899177
15	28	0.0902276
16	30	0.0936588

Curve Properties

General | Source | Info

Number of values:	16		
X-Start:	0	Y-Start:	0.0143141
X-End:	30	Y-End:	0.0958219
X-Min:	0	Y-Min:	0
X-Max:	30	Y-Max:	0.0958219

	Time	Lateral Creepage of Pearlite steel
1	0	0.0143141
2	2	0
3	4	0.00013637
4	6	0.000251396
5	8	0.000660758
6	10	0.0299601
7	12	0.0301834
8	14	1.3214e-05
9	16	0.0898169
10	18	0.0901307
11	20	4.92909e-06
12	22	0.000437663
13	24	0.0106067
14	26	0.0107728
15	28	0.0955037
16	30	0.0958219

Table C2: Longitudinal and Lateral Creep Force

Curve Properties

General | Source | Info

Number of values:	16
X-Start: 0	Y-Start: 1479.51
X-End: 30	Y-End: 132.525
X-Min: 0	Y-Min: 0
X-Max: 30	Y-Max: 2307.06

	Tme	Longitudinal Creep Force of Mn-steel
1	0	1479.51
2	2	285.605
3	4	0
4	6	1921.2
5	8	2307.06
6	10	983.965
7	12	8.77232
8	14	9.31058
9	16	9.8486
10	18	121.007
11	20	121.581
12	22	122.155
13	24	122.729
14	26	123.303
15	28	123.878
16	30	132.525

Curve Properties

General | Source | Info

Number of values:	16
X-Start: 0	Y-Start: 1085.19
X-End: 30	Y-End: 137.459
X-Min: 0	Y-Min: 0
X-Max: 30	Y-Max: 2207.89

	Time	Longitudinal Creep Force of Pearlite steel
1	0	1085.19
2	2	339.878
3	4	0
4	6	1877.64
5	8	2207.89
6	10	230.545
7	12	385.752
8	14	1833.39
9	16	34.7174
10	18	34.9561
11	20	36.3117
12	22	37.2526
13	24	2.1853
14	26	136.337
15	28	136.896
16	30	137.459

Curve Properties

General | Source | Info

Number of values: 16

X-Start:	0	Y-Start:	10.0297
X-End:	30	Y-End:	1397.37
X-Min:	0	Y-Min:	0
X-Max:	30	Y-Max:	1595.97

	Time	Lateral Creep Force of Mn-steel
1	0	10.0297
2	2	0
3	4	1595.97
4	6	1464.11
5	8	1305.79
6	10	1333.95
7	12	18.5352
8	14	32.0686
9	16	168.259
10	18	1397.35
11	20	1397.32
12	22	1397.28
13	24	1397.29
14	26	1563.34
15	28	1397.39
16	30	1397.37

Curve Properties

General | Source | Info

Number of values: 16

X-Start:	0	Y-Start:	11.8173
X-End:	30	Y-End:	1397.33
X-Min:	0	Y-Min:	0
X-Max:	30	Y-Max:	1599.05

	Time	Lateral Creep Force of Pearlite steel
1	0	11.8173
2	2	0
3	4	0.118827
4	6	2.96158
5	8	13.8964
6	10	1304.2
7	12	1245.71
8	14	1227.13
9	16	440.739
10	18	540.109
11	20	216.176
12	22	608.348
13	24	1138.93
14	26	1484.95
15	28	1599.05
16	30	1397.33